

COURT FILE NUMBER	2001-14300	Clerk's Stamp
COURT	COURT OF QUEEN'S BENCH OF ALBERTA	
JUDICIAL CENTRE	CALGARY	
APPLICANT	REBECCA MARIE INGRAM, HEIGHTS BAPTIST CHURCH, NORTHSIDE BAPTIST CHURCH, ERIN BLACKLAWS and TORRY TANNER	
RESPONDENTS	HER MAJESTY THE QUEEN IN RIGHT OF THE PROVINCE OF ALBERTA and THE CHIEF MEDICAL OFFICER OF HEALTH	
DOCUMENT	AFFIDAVIT OF KIMBERLEY SIMMONDS	
ADDRESS FOR SERVICE AND CONTACT INFORMATION OF PARTY FILING THIS DOCUMENT	Alberta Justice, Constitutional and Aboriginal Law 10 th Floor, 102A Tower 10025 -102A Avenue Edmonton, Alberta T5J 2Z2 Attn: Nicholas Parker and David Kamal Tel: (780) 643-0853; (780) 415-2993 Fax: (780) 643-0852	

**AFFIDAVIT OF KIMBERLEY SIMMONDS
AFFIRMED ON JULY 11, 2021**

I, Kimberley Simmonds, of the City of Edmonton, in the Province of Alberta, AFFIRM AND DECLARE THAT:

1. From March 2020 until March 2021, I supported Alberta's Emergency Operations Centre as the lead for analytics and modelling for Alberta's COVID-19 response.
2. I have personal knowledge of the facts and matters hereinafter deposed to by me, except where same are stated to be based upon information and belief, and those I believe to be true.

3. I have a PhD in epidemiology and my thesis combined mathematical modelling and classic epidemiology. I am an adjunct professor at the University of Calgary Cummings School of Medicine. Additional qualifications are set out in my Curriculum Vitae attached as **Exhibit A**.

4. I am an applied epidemiologist having worked in various settings from the hospital as an infection control hospital epidemiologist to leading the provincial responses to population-based outbreaks such as measles, pertussis, and more recently COVID-19. My experience working in Alberta managing outbreaks and leading infectious disease surveillance in the province over the past fifteen years is relevant experience.

5. I have made time to publish several peer reviewed papers including international collaborations with the US Centre for Disease Control (CDC) on the epidemiology of H1N1 and seasonal influenza. I have developed and used compartment models such as the Susceptible Infected-Recovered (SIR) models for both COVID-19 and influenza.

6. In addition to my work as an epidemiologist, I have worked in a senior strategic policy role for the provincial government, allowing me to understand the nuances of policy development while considering the most relevant epidemiological quantitative evidence. In 2020, I taught a course on pandemic policy development at University of Alberta.

7. Due to my expertise in infectious disease epidemiology, mathematical modelling of infectious diseases, and policy, I was asked to support Alberta's Emergency Operations Centre as the lead for analytics and modelling for the COVID-19 response.

8. The analytics team that supports the COVID-19 response grew over time but began with six epidemiologist/data analysts and one mathematical modeller (Dr Varughese). The Public Health Agency of Canada also provided one to two epidemiologists over most of the pandemic to support our more complex outbreak investigations. The mathematics department at the University of Alberta supported the lone mathematical modeller on the Alberta Health team. Over time the team expanded and there are now approximately ten staff providing analytic support.

9. Alberta's response to case identification and case management is similar to the other provincial responses, with a couple of notable exceptions. In Alberta, case identification and

management are clearly laid out in the *Alberta Public Health Disease Management Guidelines - Coronavirus -COVID-19* that is updated as new information becomes available on the situation.

A high-level overview is as follows:

- a. Identification occurs when a person has a laboratory confirmation of infection with the virus (SARS-CoV-2) that causes COVID-19.
- b. Data is electronically received from the testing laboratories in batches approximately every 10-15 minutes by the Provincial Surveillance Information (PSI) system, which is a key system used to monitor communicable diseases in the province.
- c. When contact tracers, led by Alberta Health Services, initiate a case investigation, the Communicable Disease & Outbreak Management (CDOM) system is used. The case information from CDOM is electronically submitted to Alberta Health into the Communicable Disease Reporting System (CDRS). The collected case information falls into the following broad categories: demographic, activities during the incubation period, where disease was likely acquired, activities while infectious, occupation, and disease symptoms and severity.

10. Outbreak definitions and management are laid out in the *Alberta Public Health Disease Management Guidelines -Coronavirus -COVID-19*. In Alberta, when an outbreak is suspected, the laboratory assigns an Exposure Investigation (EI) number to all laboratory requisitions and reporting. This number is attached to all cases associated with the outbreak and is useful for tracking outbreaks. Between March 11, 2020 (when a pandemic was declared) and May 15, 2021, there have been 4,746 outbreaks identified in a diverse number of settings. A non-exhaustive list of settings includes house parties, and social gatherings, congregate living, hospitals, offices, work camps, warehouses, places of worship, schools, and venues for fitness activities. Initially the most common outbreaks were in settings such as continuing care where those most vulnerable to severe outcomes as result of COVID reside, but quickly there were outbreaks in numerous settings. Attached as **Exhibit B** is an overview of outbreaks in places of worship and fitness locations in Alberta).

11. Reporting of surveillance information is critical to ensure a timely public health response. Numerous reports are produced on a regular basis to ensure that the required data and evidence is available to decision makers. In addition, ad-hoc reporting is routinely required for specific stakeholders and for Emergency Management Cabinet Committee (EMCC). Attached as **Exhibit C** is a list of daily report.

12. In order to generate the reports, there was a daily reporting workflow. The details of the workflow for case reporting is detailed in **Exhibit D**. A brief overview of the daily reporting workflow is as follows:

- a. Combine data from laboratory data (in PSI), and case and possibly outbreak information (in CDRS).
- b. Extract the required data and use two statistical software programs, SAS and R studio, to pull in chronic disease data and daily hospitalizations and perform data management queries and cleaning including duplicate check and missing Unique lifetime identifiers (ULIs).
- c. Generate the final daily file for reports and the daily dashboard.

13. Indicators were used throughout the pandemic response to provide a quick assessment of disease transmission and how well the health system was managing with the increase in COVID patients. Over time various indicators were reported to the public, but internally the following metrics were consistently reported at the zone level: lab testing positivity, active case rate, hospitalizations (including ICU), and R-value.

14. The analytics team conducted risk assessments to inform policy decisions. The team was continuously reviewing all the available data to identify key trends at the local, zonal, and provincial level, including where disease was likely acquired and what activities had the highest transmission rates. A review of the literature and experiences in other jurisdictions was often used to supplement the local evidence provided. The analytics team looked at specific locations and activities of increased transmission to provide targeted approaches to restrictions. This information was then included in the relevant reports for decision makers.

15. The role of the analytics team during the COVID response was to provide the evidence to the Chief Medical Officer of Health (CMOH) and senior leadership at Alberta Health, who in turn determined what recommendations would proceed to elected officials who were ultimately the ones responsible for making the decisions.

16. Modelling was used as a tool to forecast and assess the impact of COVID-19. Primary outcomes were cases and hospitalizations (ICU and non-ICU). Modelling was conducted using an age structured Susceptible-Infected-Recovered (SIR) compartment model and later revised to a Susceptible-Infected-Recovered-Susceptible (SIRS) model which accounted for vaccination in the population. Initial data for modelling was sparse and required significant effort to produce reasonable results as discussed in the paper found at <https://www.ncbi.nlm.nih.gov/pmc/articles/PMC7104073/>), a printout of which is attached as **Exhibit E**. However, the model did accurately predict uncontrolled spread as observed in the real-world experience in wave 2 of the pandemic in Alberta as shown in Alberta's fall predictions attached as **Exhibit F**.

17. Predictive models were used to forecast throughout the pandemic. The most common was the SIR model that is often used to predict the transmission dynamics in a population. The basic concept is that a population can be organized into one of three compartments: susceptible, infected, and recovered. At the start of an outbreak most of the population are susceptible and as the infection spreads through the population more people are infected and subsequently, they recover or die. The probability that a susceptible and an infectious individual meet and the infection is passed from the infected to the susceptible is the effective transmission rate (β). In some circumstances, a condition called endemic equilibrium occurs and the disease rate is maintained at some static rate. This is sometimes the premise for letting an infection run through a population, the notion that eventually this state of endemic equilibrium occurs. Unfortunately, for respiratory diseases like COVID-19, this does not occur if anything upsets the equilibrium. Things that disrupt the equilibrium include new variants with increased β , waning immunity, new susceptible people in the population (births, in migration), or more infected people being introduced (e.g. travel). History has shown that infectious diseases are cyclical and unable to achieve consistent endemic equilibrium. Historical data from Alberta shows a cyclical pattern of outbreaks from measles, rubella, polio, and smallpox prior to widespread vaccine availability and

subsequent herd immunity. The outbreaks occurred as soon as enough births occurred that a large enough pool of susceptible people was created to then become infected. Graphs illustrating the above described are in the linked report: (<https://open.alberta.ca/dataset/09ff0f40-1cfc-48fd-b888-4357104c3c32/resource/c5ceca04-ccda-4811-9ed0-03a3cbe8c0fb/download/7019844-notifiable-disease-incidence-1919-2014.pdf>), a printout of pages 1 to 17 of which is attached as **Exhibit G**. An endemic equilibrium state for COVID-19 is a hypothesis, however, in the real world it has not occurred.

18. In the summer of 2020, modelling work focused the transmission dynamics of COVID-19 with the population back indoors in offices and schools in the fall. Short term projections of the effects of various public health measures were evaluated to assess the change in cases/hospitalizations. Modelling predictions aligned with those from the Public Health Agency of Canada that stricter public health interventions would have the most significant effect on disease transmission rates. Short term projections were targeted to focus on the impact of COVID-19 on the acute care system to ensure there was enough health system capacity. The public health actions were to be informed by Alberta's data and experiences, up-to-date research, and experiences of other jurisdictions. The impact of proposed public health measures on transmission dynamics were assessed based on the following criteria provided to the analytics team- the goal was to protect those who are most vulnerable, tailor public health measures to local needs and circumstances as much as possible, and that consideration were made for the larger complex strategic context – health, economic, and social needs.

19. In September 2020, cases increased from the August average of 99 daily cases to 141 in September, driven by increased COVID-19 transmission in the Edmonton Zone and some rural areas, notably the City of Lethbridge and the surrounding county. This subsequently resulted in an increase in COVID-19 hospitalizations, and on October 11 Alberta's hospitalizations and ICU admissions reached a new high with 85 hospitalizations and 16 ICU admissions for a total of 101 hospitalizations including ICU. As Edmonton was experiencing a more significant level of disease transmission than the other areas of the province, voluntary measures were implemented to reduce the spread of COVID-19, specifically the potential for outbreaks and super spreader events: *residents and visitors to the zone should limit gatherings to no more than 15 people; "Wear non-medical masks in all indoor work settings, except when alone in workspaces or*

where there is adequate separation or barriers; and limit their cohorts to no more than three (a core/household cohort, a school cohort, one additional sport, social or other cohort), except young children, who can be part of four cohorts if they attend childcare". Approximately two weeks later, these voluntary measures were implemented in Calgary as well.

20. In October, daily cases continued to increase, and measures provided for Thanksgiving weekend included indoor gatherings limited to only household and cohort members. The data from Alberta and worldwide showed household transmission of COVID-19 was higher than in other settings, which follows logically as transmission is a function of exposure time, proximity to others, and use of personal protective equipment (PPE).

21. After the thanksgiving weekend, October 12, the rate of increase of new daily cases continued to rise. Edmonton remained the hotspot in the province with a weekly R_t of 1.35. The sized of the outbreaks continued to grow in acute and continuing care facilities putting pressure on the health system.

22. The number of outbreaks rose steadily in October. Indoor and household gatherings became an increasing source of transmission. Two weeks after Thanksgiving, on October 26, the new daily cases, R_t , and positivity were all higher than they had ever been before. On October 26 a mandatory 15-person limit on all social gatherings (indoor and outdoor) in the cities of Edmonton and Calgary was implemented. This limit applied to gatherings such as dinner parties, wedding and funeral receptions, banquets, and other gatherings. This excluded structured events such as dining in restaurants, theatres, worship services, or wedding and funeral ceremonies.

23. In November 2020, as expected, the hospitalizations began to rise rapidly as case growth leads to hospitalization growth, but as a lagging indicator as it takes time get sick enough to require hospitalization. A key characteristic of COVID growth is that it can turn from manageable to exponential in a matter of days to weeks. As case growth became exponential, the data obtained from contact tracing became less timely and complete. The ability to identify outbreaks and link cases to events began to deteriorate. The evidence suggested that targeted restrictions were insufficient, and that acute care would be overwhelmed. On November 24, 2020 with 1,264 new cases, 50,410 active cases in the province and 396 people in hospital and an additional 74 in the ICU, a state of public health emergency was declared.

24. In December, the focus of the analytics team was to monitor the impact of the restrictions. The short-term forecasting estimated a peak of hospitalizations the last week of December. The actual ICU peak was December 28 and non-ICU hospitalizations was two days later, December 30, 2020.

25. In January 2021, as the cases and associated hospitalizations began to decrease and vaccines were being administered to healthcare workers and those in long term care facilities, variants of concern (VOC) began to emerge worldwide. As with the previous phases of the pandemic, the data was sparse and evolving. Evidence from other jurisdictions such as the UK, and projections using Alberta data showed VOCs could out compete the wildtype. The B.1.1.7 variant was the most likely to be the dominant strain as it has a shorter incubation time and a longer infectious period. In one household in Alberta there was a two-day incubation and a parent who was isolating in the home was still able to transmit a COVID-19 VOC to a child in the home. **Exhibit H** details the epidemiology of the VOCs since their identification in Alberta.

26. In February and March, the forecasting was revised to focus on the impact of the VOC and vaccinations on hospitalizations, particularly ICU. The model estimated that the impacts of rapid immunization would not immediately reduce the hospitalizations and ICU admissions as 14-21 days is required to develop immunity. The data shows that approximately two weeks after restrictions were implemented May 5, 2021 the number of people in ICU peaked and then began to decrease.

27. The third wave began in March 2021 and was the result of the increasing variants, specifically the B.1.1.7, which has impacted younger and healthier Albertans compared to the previous waves. As more older Albertans receive the vaccine they are protected, leaving the remaining population as susceptible. At the same time, there was increasing non-compliance with following the restrictions and cases who decline to provide information to contact tracers.

28. The peak of the third wave was April 30, 2021 when 2,408 cases were identified, the highest daily case count to date, with 665 outbreaks in schools, and 6,492 associated cases as a result of the VOCs. As with the previous waves targeted measures were implemented at first. On April 29th it was announced schools would close in areas with more than 350 active cases per 100,000. Affected areas included the biggest municipalities in the province Edmonton, Calgary,

Fort McMurray, Red Deer, Grande Prairie, Lethbridge, and Airdrie. With the VOC in schools and activities surrounding schools, these had become areas of increased transmission.

- 29. In summary, in responding to the COVID-19 pandemic:
 - a. The evidence is constantly shifting. What we thought in March 2020 is different than in 2021. Scientific knowledge is not static, rather it is constantly updating based on new data. Epidemiologists use evidence, both local and from other jurisdictions to provide information to decision makers.
 - b. The data and evidence were constantly assessed and provided to elected officials to be used as part of the decision-making process.
 - c. Every time a COVID-19 transmits from one person to another, and virus replicates, there is an increasing likelihood of a new variant. Therefore, public health measures attempt to stop or slow transmission. Wave 2 allowed for uncontrolled spread which led to wave 3 driven by variants.

AFFIRMED BEFORE ME in the City)
 of Edmonton, Province of Alberta, this)
 11 day of July, 2021 I certify that)
 Kimberley Simmonds satisfied me that)
 she is a person entitled to affirm.)
)
)
 _____)
 Commissioner for Oaths in and for the)
 Province of Alberta)



 KIMBERLEY SIMMONDS

Nick Parker
Barrister & Solicitor

This is Exhibit - A referred to in the Affidavit of

Kimberley Simmonds, PhD

ADP
Allirmed

Kimberley Simmonds

Sworn before me this 11 day of July A.D., 2021

Nick Parker
Barrister/Solicitor

EDUCATION & ACADEMIC APPOINTMENTS

- o Doctor of Philosophy (PhD) 2016. University of Calgary, Department of Community Health Sciences. Thesis: *A Mathematical Model for Optimal Screening for Methicillin Resistant Staphylococcus aureus (MRSA) in Acute Care Facilities*. Doi: <http://dx.doi.org/10.11575/PRISM/24781>
- o Masters of Medical Science (MSc) 2003. University of Calgary, Department of Community Health Sciences. Thesis: *Nursing workload and its relationship to vancomycin-resistant enterococci colonization in chronic dialysis patients*. Doi: <http://dx.doi.org/10.11575/PRISM/24057>
- o Bachelor of Science (BSc) 2001. University of Calgary. Major in Cellular Molecular and Microbial Biology with a concentration on microbiology.
- o Adjunct Professor, University of Calgary, Department of Community Health Sciences, Faculty of Medicine.

EMPLOYMENT HISTORY

March 2021 - present

Senior Manager- National Health Practice, EY

- o Lead large scale client engagements and the development of complex healthcare deliverables.

March 2020 – March 2021

COVID Analytics lead, Emergency Operations Centre, Alberta Health

- o Led the modelling and analytics work for the Government of Alberta for the COVID response providing data and evidence for decision makers.

2018 – 2020

Executive Director of Health System Planning & Quality, Alberta Health

- o Executive lead for the Alberta Surgical Initiative.
- o Led the development of a Health Service Planning Framework to align policy with healthcare delivery in Alberta.
- o Co-created a patient experience and quality review.

2016 – 2018

Director, Health Evidence and Policy, Research and Innovation, Alberta Health

- o Led a data access initiative together industry, academics and government.
- o Redeveloped the provincial Health Technology Assessment (HTA) framework.

- Collaborated in industry, academic and government partnerships.
- Chaired the Health Research Ethics Harmonization committee.

2016

Director of Clinical Innovation & Strategic Foresight, Alberta Health

- Led the development of the strategic plan of the Alberta Cancer Legacy Prevention Fund, including future allocations for the fund.
- Created the Strategic Foresight plan for the Ministry.
- Engaged with Strategic Clinical Networks in Alberta to support the intersection of policy and clinical practice.

2012 – 2016

Manager Infectious Diseases Epidemiology, Alberta Health

- Project manager for the development of notifiable disease reporting system.
- Led the planning, and implementing administrative systems for surveillance.

2010 – 2012

Epidemiologist, Alberta Health Services

- Developed a province wide surveillance system for antimicrobial resistant organisms and surgical site infections.

2009 – 2010

Teaching Assistant, University of Calgary

- Taught and supported the basic infection control course (MDSC 660) for infection control professionals.

2008 – 2010

Contract Position, Alberta Health and Wellness

- Epidemiological lead for the development of province wide Clostridium difficile surveillance and integrated prenatal HIV programs.

2005 – 2008

Manager Infectious Diseases Epidemiology, Alberta Health and Wellness

- Developed standards and guidelines for Methicillin-resistant Staphylococcus aureus (MRSA) with extensive stakeholder engagement.

MEMBERSHIPS & VOLUNTEERING

- Canadian Immunization Research Network (CIRN) member
- Health Standards Organization (HSO) Acute and Surgical Care Technical Committee

- E4C--Board Member-2021-present

- Institute of Public Administration (IPAC) Edmonton Regional Group-Board Member-2017-2020
- Edmonton Humane Society-Volunteer, 2017-present
- Olympian Swim Club-Volunteer-Office Lead, 2016-2020

PUBLICATIONS

1. Savage RD, Bell CA, Righolt CH, Wilkinson K, Schwartz KL, Chen C, Bolotin S, Deeks SL, Drews SJ, Jamieson FB, Johnson C, Kwong JC, Mahmud SM, Russell ML, Simmonds KA, Svenson LW, Crowcroft NS. A multisite study of pertussis vaccine effectiveness by time since last vaccine dose from three Canadian provinces: A Canadian Immunization Research Network study. *Vaccine*. 2021 May 12;39(20):2772-2779. doi: 10.1016/j.vaccine.2021.03.031. Epub 2021 Apr 17. PMID: 33875270.
2. Regan AK, Feldman BS, Azziz-Baumgartner E, Naleway AL, Williams J, Wyant BE, Simmonds K, Effler PV, Booth S, Ball SW, Katz MA, Fink RV, Thompson MG, Chung H, Kwong JC, Fell DB. An international cohort study of birth outcomes associated with hospitalized acute respiratory infection during pregnancy. *J Infect*. 2020 Jul;81(1):48-56. doi: 10.1016/j.jinf.2020.03.057. Epub 2020 Apr 20. PMID: 32325131.
3. Crowcroft NS, Schwartz KL, Savage RD, Chen C, Johnson C, Li Y, Marchand-Austin A, Bolotin S, Deeks SL, Jamieson FB, Drews SJ, Russell ML, Svenson LW, Simmonds K, Righolt CH, Bell C, Mahmud SM, Kwong JC. A call for caution in use of pertussis vaccine effectiveness studies to estimate waning immunity: A Canadian Immunization Research Network Study. *Clin Infect Dis*. 2020 May 8:ciaa518. doi: 10.1093/cid/ciaa518. Epub ahead of print. PMID: 32384142.
4. Regan AK, Feldman BS, Azziz-Baumgartner E, Naleway AL, Williams J, Wyant BE, Simmonds K, Effler PV, Booth S, Ball SW, Katz MA, Fink RV, Thompson MG, Chung H, Kwong JC, Fell DB. An international cohort study of birth outcomes associated with hospitalized acute respiratory infection during pregnancy. *Journal of Infection*. 2020 Jul;81(1):48-56. doi: 10.1016/j.jinf.2020.03.057. Epub 2020 Apr 20. PMID: 32325131.
5. Remington TL, Osman M, Simmonds K, Charlton CL, Doucette K. Baseline assessment of and linkage to care for newly diagnosed patients with chronic hepatitis B. *Canadian Liver Journal*. 2020 Summer 3(3); 263-275. <https://doi.org/10.3138/canlivj.2019-0024>
6. Kirwin E, Varughese M, Waldner D, Simmonds K, Joffe AM, Smith S. Comparing Methods to Estimate Incremental Inpatient Costs and Length of Stay Due to Methicillin-Resistant Staphylococcus Aureus in Alberta, Canada. *BMC Health Services Research*. 2019 Oct 24;19(1):743.
7. Scott AN, Buchan SA, Kwong JC, Drews SJ, Simmonds KA, Svenson LW. Using population-wide administrative and laboratory data to estimate type- and subtype-specific influenza vaccine effectiveness: a surveillance protocol. *BMJ Open*. 2019 Sep 30;9(9):e029708.
8. Bell CA, Russell ML, Drews SJ, Simmonds KA, Svenson LW, Schwartz KL, Kwong JC, Mahmud SM, Crowcroft NE. Acellular Pertussis Vaccine Effectiveness and Waning Immunity in Alberta, Canada: 2010-2015, a Canadian Immunization Research Network (CIRN) Study. *Vaccine* 2019 Jul 9;37(30):4140-4146.
9. Lucyk K, Simmonds KA, Lorenzetti DL, Drews SJ, Svenson LW, Russell ML. The association between influenza vaccination and socioeconomic status in high income countries varies by the measure used: a systematic review. *BMC Medical Research Methodology* (2019) 19:153

10. Crowcroft NS, Schwartz KL, Chen C, Johnson C, Li Y, Marchand-Austin A, Bolotin S, Jamieson FB, Drews SJ, Russell ML, Svenson LW, Simmonds K, Mahmud SM, Kwong JC. Pertussis vaccine effectiveness in a frequency matched population-based case-control Canadian Immunization Research Network study in Ontario, Canada 2009-2015. *Vaccine*. 2019 May 1;37(19):2617-2623. doi: 10.1016/j.vaccine.2019.02.047. Epub 2019 Apr 6. PMID: 30967309.
11. Naleway AL, Ball S, Kwong JC, Wyant BE, Katz MA, Regan AK, Russell ML, Klein NP, Chung H, Simmonds KA, Azziz-Baumgartner E, Feldman BS, Levy A, Fell DB, Drews SJ, Garg S, Effler P, Barda N, Irving SA, Shifflett P, Jackson ML, Thompson MG. Estimating Vaccine Effectiveness Against Hospitalized Influenza During Pregnancy: Multicountry Protocol for a Retrospective Cohort Study. *JMIR Research Protocols*. 2019 Jan 21;8(1):e11333.
12. MacDonald SE, Russell ML, Liu XC, Simmonds KA, Lorenzetti DL, Sharpe H, Svenson J, Svenson LW. Are we speaking the same language? An argument for the consistent use of terminology and definitions for childhood vaccination indicators. *Human Vaccines & Immunotherapeutics*. 2018 Nov 20. doi: 10.1080/21645515.2018.
13. Thompson MG, Kwong JC, Regan AK, Katz MA, Drews SJ, Azziz-Baumgartner E, Klein NP, Chung H, Effler PV, Feldman BS, Simmonds K, Wyant BE, Dawood FS, Jackson ML, Fell DB, Levy A, Barda N, Svenson LW, Fink RV, Ball SW, Naleway A; PREVENT Workgroup. Influenza Vaccine Effectiveness in Preventing Influenza-associated Hospitalizations During Pregnancy: A Multi-country Retrospective Test Negative Design Study, 2010-2016. *Clinical Infectious Diseases*. 2018 Oct 11. doi: 10.1093/cid/ciy737.
14. Hermann JS, Simmonds KA, Bell CA, Rafferty E, MacDonald SE. Vaccine coverage of children in care of the child welfare system. *Canadian Journal of Public Health*. 2019 Feb;110(1):44-51. doi: 10.17269/s41997-018-0135-5.
15. Buchan SA, Booth S, Scott AN, Simmonds KA, Svenson LW, Drews SJ, Russell ML, Crowcroft NS, Loeb M, Warshawsky BF, Kwong JC. Effectiveness of Live Attenuated vs Inactivated Influenza Vaccines in Children During the 2012-2013 Through 2015-2016 Influenza Seasons in Alberta, Canada: A Canadian Immunization Research Network (CIRN) Study. *JAMA Pediatrics*. 2018 Sep 1;172(9):e181514. doi: 10.1001/jamapediatrics.2018.1514.
16. Booth S, Russell ML, McDonald BM, et al. 2514. Pediatric Medically Attended Shingles in Alberta, Canada 2016; Preliminary Results. *Open Forum Infectious Disease*. 2018;5(Suppl 1):S755-S756. Published 2018 Nov 26. doi:10.1093/ofid/ofy210.2166
17. Crowcroft NS, Johnson C, Chen C, Li Y, Marchand-Austin A, Bolotin S, Schwartz K, Deeks SL, Jamieson F, Drews S, Russell ML, Svenson LW, Simmonds K, Mahmud SM, Kwong JC. Under-reporting of pertussis in Ontario: A Canadian Immunization Research Network (CIRN) study using capture-recapture. *PLoS One*. 2018 May 2;13(5):e0195984. doi: 10.1371/journal.pone.0195984.
18. MacDonald SE, Dover DC, Hill MD, Kirton A, Simmonds KA, Svenson LW. Is varicella vaccination associated with pediatric arterial ischemic stroke? A population-based cohort study. *Vaccine*. 2018 May 11;36(20):2764-2767. doi: 10.1016/j.vaccine.2018.04.012.
19. McDonald BM, Dover DC, Simmonds KA, Bell CA, Svenson LW, Russell ML. The effectiveness of shingles vaccine among Albertans aged 50 years or older: A retrospective cohort study. *Vaccine*. 2017 Dec 15;35(50):6984-6989. doi: 10.1016/j.vaccine.2017.10.067.
20. Vrancken B, Adachi D, Benedet M, Singh A, Read R, Shafran S, Taylor GD, Simmonds K, Sikora C, Lemey P, Charlton CL, Tang JW. The multi-faceted dynamics of HIV-1 transmission in Northern Alberta: A

combined analysis of virus genetic and public health data. *Infection, Genetics & Evolution*. 2017 Aug; 52:100-105.

21. Fathima S, Simmonds KA, Drews SJ, Svenson LW, Kwong JC, Mahmud SM, Quach S, Johnson C, Schwartz KL, Crowcroft NS, Russell ML; Canadian Immunization Research Network (CIRN) Provincial Collaborative Network Vaccine Effectiveness Working Group. How well do ICD-9 physician claim diagnostic codes identify confirmed pertussis cases in Alberta, Canada? A Canadian Immunization Research Network (CIRN) Study. *BMC Health Service Research*. 2017 Jul 12;17(1):479. doi: 10.1186/s12913-017-2321-1.
22. Liu XC, Bell CA, Simmonds KA, Svenson LW, Fathima S, Drews SJ, Schopflocher DP, Russell ML. Epidemiology of pertussis in Alberta, Canada 2004–2015. *BMC Public Health*. 2017 Jun 2;17(1):539.
23. Faulder KE, Simmonds K, Robinson JL. The Epidemiology of Childhood Salmonella Infections in Alberta, Canada. *Foodborne Pathogens & Disease*. 2017 Jun;14(6):364-369.
24. Passi A, Plitt SS, Lai FY, Simmonds K, Charlton C. The Economic Impact of Prenatal Varicella Immunity Among Pregnant Women in Alberta. *Vaccine*. 2017 Jan 23;35(4):570-576.
25. Guo X, Simmonds KA, Svenson J, MacDonald SE. Do children who receive an 'early dose' of MMR vaccine during a measles outbreak return for their regularly scheduled dose? A retrospective population-based study. *BMJ Open*. 2016 Aug 31;6(8):e012803.
26. Fathima S, Simmonds K, Invik J, Scott AN, Drews S. Use of laboratory and administrative data to understand the potential impact of human parainfluenza virus 4 on cases of bronchiolitis, croup, and pneumonia in Alberta, Canada. *BMC Infectious Diseases*. 2016 Aug 11;16(1):402.
27. MacDonald SE, Bell CA, Simmonds KA. Coverage and Determinants of Uptake for Privately Funded Rotavirus Vaccine in a Canadian Birth Cohort, 2008–2013. *Pediatric Infectious Disease Journal*. 2016 Jun;35(6):e177-9.
28. Liu XC, Bell C, Simmonds KA, Svenson LW, Russell ML. Adverse events following HPV vaccination, Alberta 2006–2014. *Vaccine* 2016 Apr 4;34(15):1800-5.
29. Liu XC, Bell CA, Simmonds KA, Russell ML, Svenson LW. HPV Vaccine utilization, Alberta 2008/09–2013/14 School year. *BMC Infectious Diseases*. 2016 Jan 13;16(15).
30. Kochaksaraei SG, Castillo E, Osman M, Simmonds K, Scott AN, Oshiomogho JI, Lee SS, Myers RP, Martin SR, Coffin CS. Clinical course of 161 untreated and tenofovir-treated chronic hepatitis B pregnant patients in a low hepatitis B virus endemic region. *Journal of Viral Hepatitis*. 2016 Jan;23(1):15-22.
31. Virine B, Osiowy C, Gao S, Wang T, Castillo E, Martin SR, Lee SS, Simmonds K, van Marle G, Coffin CS. Hepatitis B Virus (HBV) Variants in Untreated and Tenofovir Treated Chronic Hepatitis B (CHB) Patients during Pregnancy and Post-Partum Follow-Up. *PLoS One*. 2015; 10(10): e0140070.
32. Adachi D, Singh AE, Read R, Simmonds K, Sikora C, Tang JW. Evolving patterns of antiretroviral drug resistance from HIV genotyping in Northern Alberta, Canada: 2007–2013, a retrospective 15 year analysis. *Journal of Clinical Virology*. 2015; 70(S1):S74.
33. Bell CA, Simmonds KA, MacDonald SE. Exploring the heterogeneity among partially vaccinated children in a population-based cohort. *Vaccine*. 2015;33(36):4572-8.
34. The Canadian Nosocomial Infection Surveillance Program. What can an audit of national surveillance data tell us? Findings from an audit of Canadian vancomycin-resistant enterococci surveillance data. *Canadian Journal of Infection Control*. Summer 2015.
35. Taylor G, Gravel D, Saxinger L, Bush K, Simmonds K, Matlow A, Embree J, Le Saux N, Johnston L, Suh KN, Embil J, Henderson E, John M, Roth V, Wong A; Canadian Nosocomial Infection Surveillance

- Program. Prevalence of antimicrobial use in a network of Canadian hospitals in 2002 and 2009. *Canadian Journal of Infectious Diseases and Medical Microbiology*. 2015; 26(2):85-9.
36. MacDonald SE, Dover DC, Simmonds KA, Svenson LW. Risk of febrile seizures after first dose of measles-mumps-rubella-varicella vaccine: a population-based cohort study. *CMAJ*. 2014;186(11):824-9.
 37. Drews SJ, Simmonds K, Usman HR, Yee K, Fathima S, Tipple G, Tellier R, Pabbaraju K, Wong S, Talbot J. Characterization of Enterovirus activity, including Enterovirus D68 in pediatric patients in Alberta, Canada: 2014. *Journal of Clinical Microbiology*. 2015; 53(3):1042-5.
 38. Matkin A, Simmonds K and Suttorp V. Measles-containing vaccination rates in southern Alberta. *Canada Communicable Disease Report*. 2014; 40(12): 236-42.
 39. Kershaw T, Suttorp V, Simmonds K and St. Jean T. Outbreak of measles in a non-immunizing population, Alberta 2013. *Canada Communicable Disease Report*. 2014; 40(12): 243-50.
 40. Chui L, Li V, Fach P, Delannoy S, Malejczyk K, Patterson-Fortin L, Poon A, King R, Simmonds K, Scott AN, Lee MC. Molecular profiling of human and cattle *Escherichia coli* O157:H7 and non-O157 strains in Alberta, Canada. *Journal of Clinical Microbiology*. 2015; 53(3):986-90.
 41. Simmonds K, Fathima S, Chui L, Lovgren M, Shook P, Shuel M, Tyrrell GJ, Tsang R, Drews SJ. Dominance of two genotypes of *Bordetella pertussis* during a period of increased pertussis activity in Alberta, Canada: January to August 2012. *International Journal of Infectious Diseases*. 2014; 29:223-5.
 42. Liu XC, Simmonds KA, Russell ML, Svenson LW. Herpes zoster vaccine (HZV): utilization and coverage 2009 - 2013, Alberta, Canada. *BMC Public Health*. 2014; 14:1098.
 43. Azevedo LC, Choi H, Simmonds K, Davidow J, Bagshaw SM. Incidence and long-term outcomes of critically ill adult patients with moderate-to-severe diabetic ketoacidosis: retrospective matched cohort study. *Journal of Critical Care*. 2014;29(6):971-7.
 44. MacDonald SE, Dover DC, Simmonds KA, Svenson LW. Risk of febrile seizures after first dose of measles-mumps-rubella-varicella vaccine: a population-based cohort study. *CMAJ*. 2014 5;186(11):824-9.
 45. Li V, Chui L, Simmonds K, Nguyen T, Golding GR, Yacoub W, Ferrato C, Louie M. Emergence of new CMRSA7/USA400 methicillin-resistant *Staphylococcus aureus* spa types in Alberta, Canada, from 2005 to 2012. *Journal of Clinical Microbiology*. 2014;52(7):2439-46.
 46. Fathima S, Ferrato C, Lee BE, Simmonds K, Yan L, Mukhi SN, Li V, Chui L, Drews SJ. *Bordetella pertussis* in sporadic and outbreak settings in Alberta, Canada, July 2004 - December 2012. *BMC Infectious Diseases*. 2014;14(1):48.
 47. Bifolchi N, Michel P, Talbot J, Svenson L, Simmonds K, Checkley S, Chui L, Dick P, Wilson JB. Weather and livestock risk factors for *Escherichia coli* O157 human infection in Alberta, Canada. *Epidemiology and Infection*. 2014;142(11):2302-13.
 48. Russell ML, Dover DC, Simmonds KA, Svenson LW. Shingles in Alberta: Before and after publicly funded varicella vaccination. *Vaccine*. 2014; 32(47):6319-24.
 49. Kopolovic I, Simmonds K, Duggan S, Ewanchuk M, Stollery DE, Bagshaw SM. Risk factors and outcomes associated with acute kidney injury following ruptured abdominal aortic aneurysm. *BMC Nephrology*. 2013; 14(1): 99.
 50. Kopolovic I, Simmonds K, Duggan S, Ewanchuk M, Stollery DE, Bagshaw SM. Elevated cardiac troponin in the early post-operative period and mortality following ruptured abdominal aortic aneurysm: a retrospective population-based cohort study. *Critical Care*. 2012; 16(4): R147.

51. Drews SJ, Lau C, Andersen M, Ferrato C, Simmonds K, Stafford L, Fisher B, Everett D, Louie M. Laboratory-based surveillance of travel-related *Shigella sonnei* and *S. flexneri* in Alberta from 2002 to 2007. *Globalization and Health*.2010; 1(6): 20-24.
52. Kim J, Ferrato C, Golding GR, Mulvey MR, Simmonds KA, Svenson LW, Keays G, Chui L, Lovgren M, Louie M. Changing epidemiology of methicillin-resistant *Staphylococcus aureus* in Alberta, Canada: population-based surveillance 2005-2008. *Epidemiology and Infection*. 2010; 139: 21:1-10.
53. Brindley PG, Simmonds MR, Needham CJ, Simmonds KA. Teaching airway management to novices: a simulator manikin study comparing the 'sniffing position' and 'win with the chin' analogies. *British Journal of Anaesthesia* .2010; 104(4): 496-500.
54. Simmonds KA, Dover DC, Louie M, Keays G. Epidemiology of community associated methicillin-resistant *Staphylococcus aureus*. *Canadian Communicable Disease Report*. 2008; 34(8): 1-9.
55. Brindley PG, Simmonds M, Meggison H, Simmonds K, Bagshaw SM. Best evidence in critical care medicine. Steroids in sepsis: bulking up the evidence. *Canadian Journal of Anaesthesia*. 2008; 55(9): 648-50.

COVID-19 – Outbreaks

Places of Worship Outbreaks

There have been 35 outbreaks identified that are associated with places of worship between March 1, 2020-May 15, 2021 with a total of 704 directly associated cases. When separate outbreaks are spawned from the places of worship outbreaks, the secondary outbreak cases are not counted towards the place of worship outbreak.

Date Opened	Outbreak Number	Cases	Variant of concern	Zone
2020-03-19	2020-CAL-A058	21	0	Calgary
2020-03-31	2020-CAL-A072	27	0	Calgary
2020-08-15	2020-EI-3563	105	0	Edmonton
2020-08-15	2020-EI-3561	19	0	North
2020-08-27	2020-EI-3813	167	0	Calgary
2020-10-07	2020-EI-4705	9	0	Edmonton
2020-11-08	2020-EI-5851	11	0	Edmonton
2020-11-14	2020-EI-5960	12	0	Calgary
2020-11-17	2020-EI-6062	2	0	Calgary
2021-01-08	2021-EI-242	8	0	South
2021-01-27	2021-EDM-B111	17	0	Edmonton
2021-02-05	2021-EI-1245	8	7	Central
2021-02-16	2021-EI-1637	11	0	Calgary
2021-02-25	2021-EI-1983	2	0	Calgary
2021-03-15	2021-EI-2771	24	23	South
2021-04-02	2021-EI-3664	7	0	Calgary
2021-04-09	2021-EI-4042	5	5	Edmonton
2021-04-09	2021-EI-4056	18	15	Central
2021-04-14	2021-EI-4354	5	0	Calgary
2021-04-14	2021-EI-4357	5	5	Central
2021-04-14	2021-EI-4370	10	0	North
2021-04-14	2021-EI-4363	7	7	Edmonton
2021-04-15	2021-EI-4418	11	11	Central
2021-04-20	2021-EI-4764	5	0	Edmonton
2021-05-07	2021-EI-6011	8	7	Calgary
2021-05-08	2021-EI-6099	9	3	Central

This is Exhibit ^B referred to in the
Affidavit of
Kimberley Simmonds
Sworn before me this 11th day
of July A.D., 2021

A Notary Public, A Commissioner for Oaths
in and for the Province of Alberta

Nick Parker
Barrister & Solicitor

COVID-19 – Outbreaks

Sports and Fitness Facility Outbreaks

There have been thirty-three outbreaks associated with Sports and Fitness Facilities between March 1, 2020-May 15, 2021 with a total of 501 directly associated cases. When separate outbreaks are spawned from the fitness outbreaks, the secondary outbreak cases are not counted towards the fitness outbreak. The overall attack rates at fitness facilities and within sport cohorts have an average attack rate of 24 percent, but some outbreaks have had attack rates as high as 46 per cent. Fitness outbreaks have been reported in all zones in the province.

Date Opened	Outbreak Number	Cases	Variant of concern	Zone
2020-07-17	2020-EI-2993	65	0	Calgary
2020-10-07	2020-EI-4709	41	0	Edmonton
2020-10-12	2020-EI-4859	13	0	Edmonton
2020-10-18	2020-EI-5049	6	0	Calgary
2020-10-29	2020-EI-5408	18	0	Edmonton
2020-11-02	2020-EI-5495	13	0	Calgary
2020-11-03	2020-EI-5559	17	0	Calgary
2020-11-04	2020-EI-5575	14	0	North
2020-11-10	2020-EI-5778	8	0	South
2020-11-12	2020-EI-5874	7	0	Calgary
2020-11-13	2020-EI-5936	6	0	Central
2020-11-15	2020-CAL-A108	7	0	Calgary
2020-11-16	2020-EI-6034	17	0	Calgary
2020-11-18	2020-EI-6159	12	0	Edmonton
2020-11-22	2020-EDM-B076	4	0	Edmonton
2020-11-28	2020-CAL-A114	24	0	Calgary
2020-11-29	2020-NOR-C055	4	0	North
2020-11-30	2020-CEN-202	8	0	Central
2020-12-01	2020-EI-6792	9	0	Calgary
2020-12-05	2020-EI-6991	3	0	North
2020-12-06	2020-EI-7002	10	0	Central
2021-02-09	2021-EI-1391	8	0	Calgary
2021-03-17	2021-EI-2840	5	0	Calgary
2021-03-18	2021-EI-2919	7	7	Calgary
2021-03-19	2021-EI-2969	17	13	Calgary
2021-03-24	2021-CAL-A006	6	0	Calgary
2021-03-27	2021-EI-3384	6	2	Calgary
2021-03-28	2021-EI-3420	35	34	Calgary
2021-04-12	2021-CEN-021	73	25	Central
2021-04-20	2021-EI-4743	14	13	Edmonton
2021-04-23	2021-EI-5049	11	9	Calgary
2021-04-25	2021-EI-5133	7	7	Central
2021-04-26	2021-EI-5218	6	5	Edmonton

COVID-19 – Outbreaks

Example of a Dance Studio outbreak

Outbreak index case is likely an instructor who was infected at a restaurant outbreak. 11 students infected with a VOC, and at least 32 close contacts, plus 7 students who subsequently attended school while infectious. Instructors are masked, students attend in cohorts, distanced but unmasked. Room is cleaned between groups. Studio is 1500sqft with 20ft ceilings. There are multiple secondary transmissions (infected close contacts), but not quantified here.



 Date owner of dance studio was finally reached. Owner unaware of other positive individuals at this time.

 Date outbreak investigation launched.

+Close contacts are household + other

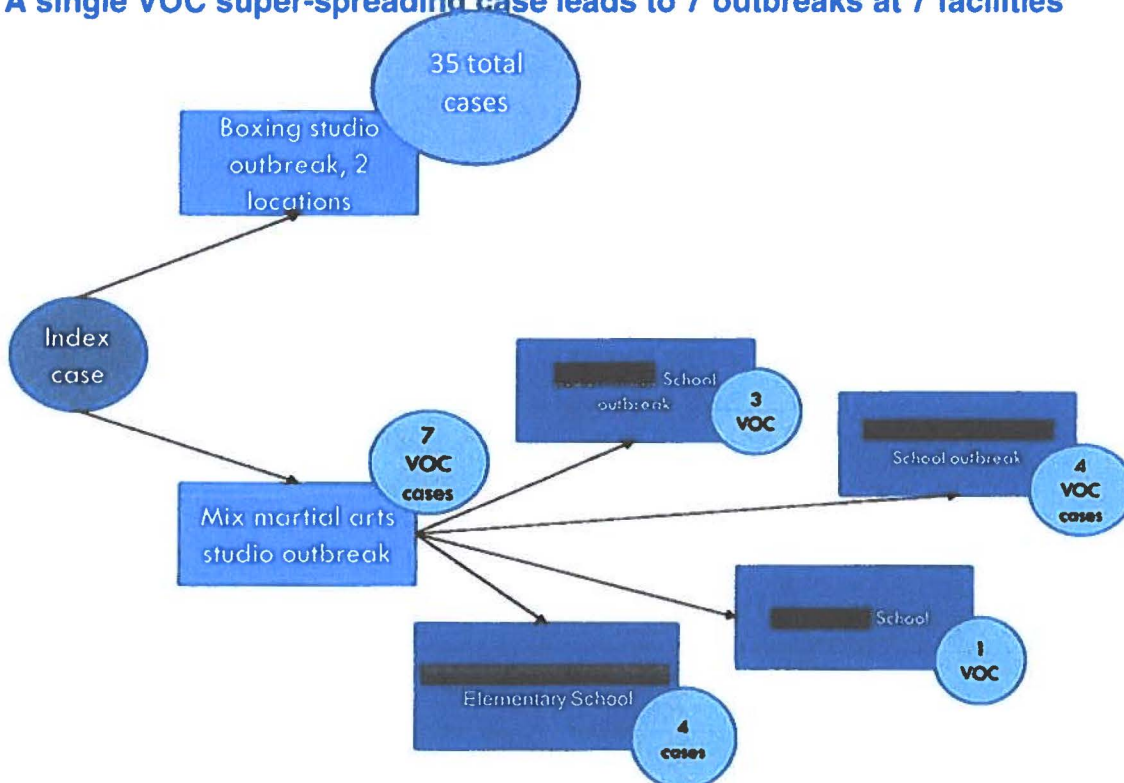
	Close Conta cts*	Scho ol while infec tious	Da y 1	Da y 2	Da y 3	Da y 4	Da y 5	Da y 6	Da y 7	Da y 8	Da y 9	Da y 10	Da y 11	Da y 12	Da y 13	Da y 14	Da y 15	Da y 16	Da y 17	Da y 18
Instruc tor	1+0	n/a	Blue			Blue	Blue	Blue	Blue	Blue	Black		Blue			Red				
Stude nt 1	4+1	yes				Blue	Blue	Blue	Blue	Blue			Blue	Green						
Stude nt 2	2+3	no	Blue	Blue		Blue	Blue	Blue	Blue		Red	Blue	Blue	Green						
Stude nt 4	2+1	no			Blue	Blue	Blue	Blue	Blue	Blue	Blue	Red	Green							
Stude nt 5	3+3	yes			Blue	Blue	Blue	Blue	Blue			Red	Green							
Stude nt 3	3+0	yes				Blue	Blue	Blue	Blue	Light Blue			Red	Green						
Stude nt 6	3+0	no		Blue	Blue	Blue	Blue	Blue	Blue				Red	Green						
Stude nt 11	4+0	no												Red		Green				
Stude nt 8	?	yes						Blue					Blue		Red					
Stude nt 7	?	yes	Blue		Blue	Blue	Blue	Blue		Blue						Red	Green			
Stude nt 9	?	yes				Blue	Blue	Blue									Red	Green		
Stude nt 10	3+0	yes				Blue								Blue				Red		

COVID-19 – Outbreaks

Boxing Studio- Mixed Martial Arts School- School Cluster

This outbreak began as part of a B.1.1.7 UK variant super-spreader cluster in Calgary in which one individual was infectious for 6 days prior to his symptom onset date and attended two boxing gyms. This facility has two locations, and COVID has been transmitted at both facilities. High intensity exercise was taking place despite restrictions. For a time at the beginning of the outbreak, no masking was occurring during weight training. Sparring was occurring at the facility, while masking was in place, clearly distancing was not possible. Disinfection was also inadequate and often there was less than 3m distancing between patrons. Additionally, no health screening was in place for staff. Currently there are 35 cases between these two locations.

A single VOC super-spreading case leads to 7 outbreaks at 7 facilities



COVID Response – Daily Reporting
May 2021

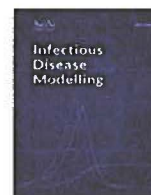


Report	Purpose	Report sent to:	Frequency	Time of Day	Lead
Morning ballpark from Analytics	Initial estimate of daily cases, lab tests, and positivity rate. Also includes active case estimates and VOC's.	CMOH, Incident Commander, ADM	Daily (M-S)	8:00AM	Data & Analytics
Health Surveillance Epidemiology Report	Full scale daily epidemiology report – for internal use.	All EOC staff and key contacts	Daily (M-F)	Noon	Data & Analytics
Health Surveillance External Report	Daily reporting for external posting/use.	Communications, AHS, External contacts	Daily (M-F)	Noon	Data & Analytics
Health Minister Situation Report	Daily sitrep including case counts, outbreaks, immunization data, VOC's and any other pertinent information.	Sent to EOC for formatting and sending to distribution list including Minister of Health and all EMCC members	Daily (M-F)	2:00PM Sent to distribution list at 2:30pm by AHWEOC	Data & Analytics Operations & Logistics
Daily DM Report (Outbreaks)	Outbreak information for continuing care, long term care and supported independent living.	Deputy Minister	Daily (M-F)	2:00PM	Data & Analytics
Immunization Report	Daily immunization rates for the province.	DCMOH, Section Chiefs, Communications	Daily (M-F)	Noon	Data & Analytics
First Nations Report	Cases, outbreaks, and VOC's tracking for First Nations. Provided to MOH, AHS, FNIHB, AFNIGC, Treaty 8, Stoney Nakoda Tsuut'ina Tribal Council, and other First Nations communities.	Included in EOD report that is sent to Deputy Minister	Weekly (Wednesdays)	End of Day	Data & Analytics

AP
Approved
Kimberley Simmonds
Minister of Health
21 July
11th day
A.D. 2021
referred to in the Affidavit of
Kimberley Simmonds
with Parker & Simmonds Solicitors
Minister of Health
Kimberley Simmonds

COVID Response – Daily Reporting
May 2021

Immunization Report	Detailed daily immunization rates for the province. Reconciliation and repackaging of Analytics Immunization Report; Vaccine Distribution Report; Appointments projection;	Deputy Minister	Daily (M-S)	14:00	EOC Operations / Logistics Section
Immunization details for public posting	Summary of daily immunization rates for the province.	EOC and Communications.	Daily (M-S)	14:00	EOC Operations / Logistics Section
CMOH Order Enforcement Dashboard	Dashboard of CMOH Order Enforcement actions by week.	Incident Commanders	Weekly (Typically Wednesday)	N/A	EOC Operations / Logistics Section
Vaccine appointments / utilization projection	Short-term projection of AHS and Pharmacy vaccine appointments (2 weeks)	Deputy Minister	On Demand (Typically Daily)	N/A	EOC Operations / Logistics Section
Vaccine Planning Workbook	Medium-term projection of vaccine utilization and immunization program based on known and anticipated supply; capacity to administer; and vaccination targets (1 Quarter).	Deputy Minister	On Demand (Typically weekly)	N/A	EOC Operations / Logistics Section
End of Day Report	Summary of EOC daily activities.	Deputy Minister	Daily (M-F)	8:00PM	EOC Operations / Logistics Section



Why is it difficult to accurately predict the COVID-19 epidemic?



Weston C. Roda^a, Marie B. Varughese^b, Donglin Han^a, Michael Y. Li^{a,*}

^a Department of Mathematical and Statistical Sciences, University of Alberta, Edmonton, Alberta, T6G 2G1 Canada

^b Analytics and Performance Reporting Branch, Alberta Health, Edmonton, Alberta, T5J 2N3, Canada

ARTICLE INFO

Article history:

Received 4 March 2020

Accepted 16 March 2020

Available online 25 March 2020

Handling Editor: Dr. J Wu

Keywords:

COVID-19 epidemic in Wuhan

SIR and SEIR models

Bayesian inference

Model selection

Nonidentifiability

Quarantine

Peak time of epidemic

ABSTRACT

Since the COVID-19 outbreak in Wuhan City in December of 2019, numerous model predictions on the COVID-19 epidemics in Wuhan and other parts of China have been reported. These model predictions have shown a wide range of variations. In our study, we demonstrate that nonidentifiability in model calibrations using the confirmed-case data is the main reason for such wide variations. Using the Akaike Information Criterion (AIC) for model selection, we show that an SIR model performs much better than an SEIR model in representing the information contained in the confirmed-case data. This indicates that predictions using more complex models may not be more reliable compared to using a simpler model. We present our model predictions for the COVID-19 epidemic in Wuhan after the lockdown and quarantine of the city on January 23, 2020. We also report our results of modeling the impacts of the strict quarantine measures undertaken in the city after February 7 on the time course of the epidemic, and modeling the potential of a second outbreak after the return-to-work in the city.

© 2020 The Authors. Production and hosting by Elsevier B.V. on behalf of KeAi Communications Co., Ltd. This is an open access article under the CC BY-NC-ND license (<http://creativecommons.org/licenses/by-nc-nd/4.0/>).

1. Introduction

In early December 2019, a novel coronavirus, later labelled as COVID-19, caused an outbreak in the city of Wuhan, Hubei Province, China, and it has further spread to other parts of China and many other countries in the world. By January 31, the global confirmed cases have reached 9,776 with a death toll of 213, and the WHO declared the outbreak as a public health emergency of international concern (WHO, 2020). By February 9, the global death toll has climbed to 811, surpassing the total death toll of the 2003 SARS epidemic, and the confirmed cases continued to climb globally. As governments and public agencies in China and other impacted countries respond to the outbreaks, it is crucial for modelers to estimate the severity of the epidemic in terms of the total number of infected, total number of confirmed cases, total deaths, and the basic reproduction number, and to predict the time course of the epidemic, the arrival of its peak time, and total duration. Such information can help the public health agencies make informed decisions.

* Corresponding author.

E-mail addresses: wroda@ualberta.ca (W.C. Roda), marie.varughese@gov.ab.ca (M.B. Varughese), donglin3@ualberta.ca (D. Han), myli@ualberta.ca (M.Y. Li).

Peer review under responsibility of KeAi Communications Co., Ltd.

<https://doi.org/10.1016/j.idm.2020.03.001>

2468-0427/© 2020 The Authors. Production and hosting by Elsevier B.V. on behalf of KeAi Communications Co., Ltd. This is an open access article under the CC BY-NC-ND license (<http://creativecommons.org/licenses/by-nc-nd/4.0/>).

This is Exhibit "E" referred to in the Affidavit of Kimberley Simmonds Affirmed before me this 11th day of July, 2021

Since the start of the outbreak in Wuhan, several modeling groups around the world have reported estimations and predictions for the COVID-19 (formerly called 2019-nCov) epidemic in journal publications or on websites, for an incomplete list see (Bai et al., 2020; Imai, Dorigatti, Cori, Riley, & Ferguson, 2020; Read, Bridgen, Cummings, Ho, & Jewell, 2020; Shen, Peng, Xiao, & Zhang, 2020; Tang et al., 2020b, a; Wu, Leung, & Leung, 2020; You et al., 2020; Yu, 2020; Zhao et al., 2020). The modeling results have shown a wide range of variations (Cyranoski, 2020): estimated basic reproduction number varies from 2 to 6, peak time estimated from mid-February to late March, and the total number of infected people ranges from 50,000 to millions. Why is there such a wide variation in model predictions, even among predictions made using transmission models based on either the SIR or SEIR framework? We attempt to address this variability issue in our study.

A simple answer for the wide range of model predictions might be that there was too little information at the beginning of the outbreak, especially before January 23 when Wuhan was quarantined and locked down, and that there was a lack of reliable data, except for the confirmed case data that could be used for model calibration. Rigorous model calibration methods, including maximum likelihood methods and the Bayesian inference based MCMC methods, already take into consideration uncertainties in data by allowing the data at each time point to follow a probability distribution with the mean given by the assumed model and the variance τ given by the assumed probability distribution, where the variance may depend on the mean. The lack of data, as we will demonstrate, is a more serious concern for modellers. A key issue that can explain the variability in model predictions is understanding how the available data (confirmed cases) compares with model predictions. Confirmed cases are people with symptoms who made contact with a hospital, got tested, and whose infection of COVID-19 was confirmed by DNA or imaging tests. The infected compartment in by transmission models represents all people who are infected. These include people who may or may not have symptoms and contacts with a hospital, as well as people with confirmed laboratory tests and those who are misdiagnosed. In this sense, confirmed cases (data) are only a fraction of the total infected population (model predictions). A metaphor of an iceberg best represents the difference between data and model predictions. The entire iceberg represents the total infected population, and the tip of the iceberg above the sea surface represents the case data. The part of the iceberg hidden under the water represents the infected people that are unknown to public health surveillance and testing; often called the hidden epidemic. The difference between cases and infections can be measured by the case-infection ratio ρ , between the newly confirmed cases and the number of infected people, or as a surrogate, the ratio between the cumulative confirm cases and the cumulative number of infected people.

The case-infection ratio ρ can vary widely for different viral infections that spread through air droplets and close contacts. For the SARS epidemic, the ratio ρ was in the range of $1/5 - 1/2$ (Chowell et al., 2004; Gumel et al., 2004; Lipsitch et al., 2003; Zhang et al., 2005). In contrast, for seasonal influenza in 2019–2020, the ratio ρ can be as small as $1/100$, based on estimates from the US CDC (US CDC, 2020). Why should this be a problem for the modellers? In model calibration, in order to estimate key model parameters such as the transmission rate β , by fitting the model output to the confirmed cases data, it is necessary to discount the total number of infectious people, $I(t)$, from the model prediction, by the case-infection ratio ρ to appropriately predict confirmed case data. For each value of the ratio ρ , a corresponding value for the transmission rate β can then be estimated by fitting the model to data, which in turn determines the basic reproduction number \mathcal{R}_0 , the scale of the epidemic, as well as the peak time. Given the potential wide range for the case-infection ratio ρ of the COVID-19, the estimated transmission rate β has a wide range, and hence the wide range of reported model predictions.

In modeling terms, given the confirmed-case data, there is a linkage between the model parameter ρ and the transmission rate β , and potentially also with other model parameters. While many different combinations of ρ and β can show good fit to the data, they can produce very different model predictions of the epidemic. This is known as *nonidentifiability* in the modeling literature, see e.g. (Lintusaari, Gutmann, Kaski, & Corander, 2016; Raue et al., 2009; van der Vaart, 1998). It means that a group of model parameters can not be uniquely determined from the given data during model calibration. Different choices of parameter values with the same good fit to the data can lead to very different model predictions. The ways in which nonidentifiability is addressed in the model calibration process greatly influences the reliability of model predictions.

The standard nonlinear least squares method is known to be ill suited to detect or address the nonidentifiability issue, since it relies on a rudimentary optimization algorithm. These rudimentary optimization algorithms attempt to find a global minimum of the given objective function, but there are infinitely many global minima given nonidentifiability. Standard Markov chain Monte Carlo (MCMC) procedures based on Bayesian inference often fail to converge to the target posterior distribution in the presence of nonidentifiability, and can produce best-fit parameter values with unreliable credible intervals, since these often relies on elementary MCMC algorithms. Elementary MCMC algorithms converge very slowly given a very skewed posterior distribution. In our study, we used an improved model calibration method using Bayesian inference and affine invariant ensemble MCMC algorithm that can ensure fast convergence to the target posterior distribution when facing nonidentifiability, and provide more reliable credible intervals and model predictions.

Another important factor that can significantly influence model predictions is the choice of a suitable model to describe the epidemic under study: a more complex or simpler model. A complex model incorporates more biological and epidemiological information about the epidemic and is more biologically realistic. A drawback of a complex model is that it requires more model parameters to be estimated compared to a simpler model. Given the dataset, such as the confirmed case data of COVID-19, increased number of parameters in a complex model that are unknown and need to be estimated by model fitting can lead to a greater degree of uncertainty in model predictions. In choosing an appropriate model, it is important to draw a balance between biological realism and reducing uncertainty in model predictions, and this choice can significantly influence the reliability of model predictions. The modeling procedure to determine the right balance is model selection using various information criteria, for instance the Akaike Information Criteria (AIC) for nested models (Akaike, 1973; Sugiura, 1978).

In our study, we considered both SEIR and SIR models for model predictions and applied model-selection analysis. For the given dataset of confirmed cases, we determined that the SIR model is a better choice than the SEIR model, and more likely than models that are more complex than an SEIR model (Section 3). Our study focused on the development of the outbreak in Wuhan city after the quarantine and lockdown (January 23, 2020), given the reliability of confirmed case data and definition during this period and the simplicity in our predictions and analysis. We briefly outline in Section 2 the methodology for model calibration using an improved procedure based on Bayesian inference and model selection method using Akaike Information Criteria. In Section 4, using the SIR model, we illustrate the linkage between the transmission rate and case-infection ratio, and the presence of nonidentifiability when only the confirmed-case data is used for model calibration. In Section 5, we present detailed results of the SIR model calibration and our model predictions, including the distribution of peak time, prediction interval of future confirmed cases, as well as the total number of infected people. In Section 6, we estimate the impact of further control measures recommended in Wuhan after February 7 and predicted the changes in peak time under different assumptions on the reduction of transmission achieved by these measures. In Section 7, we estimated the impact of timing the return to work on the course of the epidemic, in terms of peak time, peak values, and the duration of the epidemics. Our results are summarized in Section 8.

2. Model calibration and model selection

In this section, we give a brief description of a model calibration method based on Bayesian inference and the method of model selection using Akaike Information Criterion (AIC). For more details the reader is referred to (Portet, 2020; Roda, 2020). Other model calibration procedures using nonlinear squares or more general maximum likelihood methods are not described here, and we refer the reader to (Rossi, 2018). Model selection methods using other information criteria can also be used, see e.g. (Burnham & Anderson, 2002).

2.1. Affine invariant ensemble Markov chain Monte Carlo algorithm for model calibration

Mathematical Model. Consider a mathematical model given by a system of differential equations:

$$x' = f(x), \tag{1}$$

where $x = (x_1, \dots, x_k)$ denotes the vector of state variables, $f(x) = (f_1(x), \dots, f_k(x))$ the vector field. We let $u \in \mathbb{R}^{n_1}$ be the vector of all model parameters, which often include initial conditions $x_0 = (x_{01}, \dots, x_{0k})$. We assume that there exists a unique solution $x = x(u, t)$ for each given u .

Data. Data is often given on the observable quantities, such as newly confirmed cases, which are linear or nonlinear combinations of the solutions $x(u, t)$ in the form:

$$y = y(w, t) = y(x(u, t), v),$$

where $v \in \mathbb{R}^{n_2}$ are parameters in the observables y and $w = (u, v) \in \mathbb{R}^n$, $n = n_1 + n_2$, is the vector of all model parameters to be estimated. Furthermore, the dataset is collected at N time points t_1, t_2, \dots, t_N . We will fit the model outputs

$$y_i = y(w, t_i) = y(x(u, t_i), v), \quad i = 1, 2, \dots, N,$$

to the time series dataset

$$D = \{D_1, D_2, \dots, D_N\}.$$

Likelihood functions. In order to account for noise in the data, we let the probability of observing D_i at time t_i be given by $f_i(D_i)$, with mean y_i and variance $q_i = \sigma_i^2 = 1/\tau_i$, $i = 1, 2, \dots, N$. Common probability distributions used for this purpose include the normal distribution, Poisson distribution, and negative binomial distribution. In our Bayesian inference, the variance $q_i = 1/\tau_i$ in the noise distribution is also estimated from the data, giving us an accurate posterior distribution and accurate credible intervals for the estimated parameters. The entire set of parameters to be estimated includes model parameters u , parameters v in the observable function y , and the variances $q = (1/\tau_1, 1/\tau_2, \dots, 1/\tau_N)$, and is denoted by

$$\theta = (u, v, q).$$

We consider the likelihood function

$$L(\theta) = CP(D|\theta) = C f_1(D_1) f_2(D_2) \dots f_N(D_N),$$

where C is a constant independent of θ used to simplify the likelihood function (Kalbfleisch, 1979).

Bayesian framework. The Bayesian framework assumes that a probability model for the observed data D given unknown parameters θ is $P(D|\theta)$, and that θ is randomly distributed from the prior distribution $P(\theta)$. Statistical inference for θ is based on the posterior distribution $P(\theta|D)$. Using Bayes Theorem we obtain

$$P(\theta|D) = \frac{P(D|\theta)P(\theta)}{P(D)} = \frac{P(D|\theta)P(\theta)}{\int_{\Omega} P(D|\theta)P(\theta)d\theta} \propto L(\theta)P(\theta) = \pi(\theta|D),$$

where Ω is the parameter space of θ and $L(\theta)$ is the likelihood function. Constant $P(D) = \int_{\Omega} P(D|\theta)P(\theta)d\theta$ is used to normalize the posterior distribution $P(\theta|D)$ (Chen, Shao, & Ibrahim, 2000). The unnormalized posterior distribution is given by $\pi(\theta|D) = L(\theta)P(\theta)$. The Bayesian framework is very useful for statistical inference that occurs in mathematical modeling since it allows utilization of the prior information about the unknown parameters in the literature. Epidemiological information about the infectious disease can often inform a general range for the parameters to be estimated, and the uniform distribution is typically chosen as the prior distribution in such a case.

Markov chain Monte Carlo algorithms. Markov chain Monte Carlo (MCMC) algorithms are used to approximate a posterior distribution of parameters by randomly sampling the parameter space (Lynch, 2007). In MCMC algorithms, a new vector of parameter values $\theta^{(t)}$ is sampled iteratively from the posterior distribution, based on the previous vector $\theta^{(t-1)}$, until a sample path (also called a chain or walker) has arrived at a stationary process and produces the target unnormalized posterior distribution. Commonly used MCMC algorithms include the Metropolis-Hastings algorithm and Random-Walk Metropolis-Hastings algorithms (Chen et al., 2000).

In our study, we used an improved MCMC algorithm, the *affine invariant ensemble Markov chain Monte Carlo algorithm*, which has been shown to perform better than Metropolis-Hastings and other MCMC algorithms, especially in the presence of nonidentifiability. The algorithm uses a number of walkers and the positions of the walkers are updated based on the present positions of all walkers. For details on this algorithm, we refer the reader to (Goodman & Weare, 2010; May, 2015) and recent lecture notes on this topic (Roda, 2020).

2.2. Method of model selection using Akaike information criterion

When using mathematical models to explain data that has been formed by an underlying disease process, the principle of parsimony should be used to select a suitable model. A parsimonious model is the simplest model with the least assumptions and variables but with the greatest explanatory power for the disease process represented by the data (Johnson & Omland, 2015). This principle is also reflected in a well known quotation: “Models should be as simple as possible but not simpler.” This quotation is often ascribed to A. Einstein. The model selection method using Akaike Information Criterion takes into account both how well the model fits the data and the principle of parsimony.

Akaike Information Criterion (AIC). Let $L(\hat{\theta}_{MLE})$ be the maximum likelihood value achieved at a best-fit parameter value $\hat{\theta}_{MLE}$. Let K be the number of parameters to be estimated in a model, and N be the number of time points where data are observed. The *Akaike Information Criterion* (AIC) is defined as (Akaike, 1973):

$$AIC = -2\ln(L(\hat{\theta}_{MLE})) + 2K.$$

This definition should be used when $K < N/40$, namely when the number of time points N is large in comparison to the number of parameters. When $K > N/40$, namely when the number of parameters is large in comparison to the number of time points, the following corrected AIC should be used (Sugiura, 1978):

$$AIC_c = AIC + \frac{2K(K+1)}{N-K-1}.$$

We note that in the Bayesian inference based calibration, the unnormalized posterior distribution $\pi(\theta|D)$ is equal to the product of the likelihood function $L(\theta)$ and the prior distribution $P(\theta)$. The Akaike information criterion can be applied if uniform prior distributions are used for each parameter, since $\pi(\hat{\theta}_{MLE}) = \gamma L(\hat{\theta}_{MLE})$, where γ is a constant.

Model selection using AIC. When several nested models, each having a different level of complexity, are considered as candidates for the most suitable model, AIC values can be computed for each model, and the model associated with the smallest AIC value is considered the best model. The difference of AIC_{*i*} value of model *i* with the minimum min_{*i*}AIC_{*i*}:

$$\Delta_i = AIC_i - \min_j AIC_j.$$

This measures the information lost when using model *i* instead of a model with the smallest AIC value. When Δ_i is larger, model *i* is less plausible.

Useful guidelines for interpreting Δ_i for nested models are as follows (Burnham & Anderson, 2002):

- If $1 \leq \Delta_i \leq 2$, model *i* has substantial support and should be considered.

- If $4 \leq \Delta_i \leq 7$, model i has less support.
- If $\Delta_i > 10$, model i has no support and can be omitted.

When a large number of models are under consideration or the models are not nested, the model selection rules are different. We refer the reader to recent lecture notes (Portet, 2020) for an introduction to model selection.

3. Model selection analysis for an SEIR and an SIR model

We used both SEIR and SIR frameworks to model the COVID-19 epidemic in Wuhan, and we applied model selection analysis to decide which framework is more parsimonious.

3.1. The models

In our SIR and SEIR models, the compartment S denotes the susceptible population in Wuhan, compartment I denotes the infectious population, and R denotes the confirmed cases. In the SEIR model, a latent compartment E is added to denote the individuals who are infected but not infectious. The latency of COVID-19 infection is biologically realistic due to an incubation period as long as 14 days; newly infected individuals may not be infectious while the virus is incubating in the body. Here we note the difference between the latent period, which is the period from the time an individual is infected to the time the individual is infectious, and the incubation period, which is the period between the time an individual is infected to the time clinical symptoms appear, which include fever and coughing for COVID-19. For SARS, infected individuals become infectious on average two days after the onset of symptoms WHO (2003); so, the SARS latent period is on average longer than the incubation period. For COVID-19, evidence has shown that infected individuals can be infectious before the onset of symptoms (Bai et al., 2020), but the length of the latent period is largely unknown. In comparison to the SIR model, the SEIR model has the strength of being more biologically realistic, but the SEIR model has the drawback of having two additional unknown parameters: the latent period and the initial latent population.

The transfer diagrams for both models are shown in Fig. 1. The biological meaning of all model parameters are given in Table 1 and Table 2. A key assumption in both models is that deaths occurring in the S , E , and I compartments are negligible during the period of model predictions.

(4 months). Since we use the newly confirmed case data for model calibration, which is matched to the ρI term in both models, the death term in the R compartment has no effect on our model fitting. The systems of differential equations for each model is given below:

$$\begin{aligned} S' &= -\beta IS \\ I' &= \beta IS - (\rho + \mu)I \\ R' &= \rho I - dR \end{aligned} \tag{2}$$

$$\begin{aligned} S' &= -\beta IS \\ E' &= \beta IS - \epsilon E \\ I' &= \epsilon E - (\rho + \mu)I \\ R' &= \rho I - dR \end{aligned} \tag{3}$$

3.2. Model calibration from the data

For data reliability, the data used for both models (2) and (3) is the newly confirmed cases in Wuhan city from the official reports from January 21 to February 4, 2020 (National Health Commission of the People’s Republic of China, 2020). It is common to use a Poisson or negative binomial probability model for observed count data. When the mean of a Poisson or negative binomial distribution is large, it approximates a normal distribution. Since the newly confirmed cases are approaching large values quickly, the distribution of the count data will be approximately normal and the probability model for the observed count data in our study was assumed to a normal distribution with mean given by ρI and variance given by $1/\tau$. There are four parameters to be estimated in the SIR model from data: transmission rate β , diagnosis rate ρ , the initial population size I_0 for the compartment I on January 21, 2019 ($t = 0$), and the variance $q = 1/\tau$ for the noise distribution in the

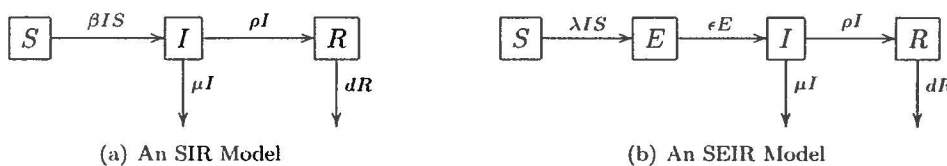


Fig. 1. Transfer diagrams for an SIR and an SEIR model for COVID-19 in Wuhan.

Table 1
Parameters in the SIR model (2) and their estimations from the confirmed case data.

	Epidemiological Meaning	Best-fit Value	95% Credible Interval	Prior
β	Transmission rate	9.906e-8	(7.02e-8, 2.09e-7)	$U(1e-10, 1e-5)$
ρ	Diagnosis rate	0.24	(0.064, 0.901)	$U(0.01, 1)$
μ	Recovery rate	0.1	fixed value	source (You et al., 2020)
I_0	Size of I on 01/20/2020	245	(65, 890)	$U(1, 8400)$
τ	$1/\tau$ is the variance of data noise	2.62e-5	(1.43e-5, 4.33e-5)	$U(1e-8, 100)$

Table 2
Parameters in the SEIR models and their estimations from the confirmed case data.

	Epidemiological Meaning	Best-fit Value	95% Credible Interval	Prior
β	Transmission rate	8.68e-8	(8.20e-8, 1.26e-7)	$U(1e-10, 1e-5)$
ρ	Diagnosis rate	0.018	(0.016, 0.024)	$U(0.01, 1)$
μ	Recovery rate	0.1	fixed value	source (You et al., 2020)
e	Transfer rate from E to I	0.631	(0.263, 0.78)	$U(0.07, 1)$
E_0	Size of E on 01/20/2020	1523	(3444, 4682)	$U(1, 1700)$
I_0	Size of I on 01/20/2020	3746	(3278, 4171)	$U(3200, 6700)$
τ	$1/\tau$ is the variance of data noise	2.61e-5	(1.43e-5, 4.13e-5)	$U(1e-8, 100)$

data. There are six parameters to be estimated for the SEIR model: transfer rate e from E to I , the initial population size E_0 for the latent compartment E on January 21, 2019, and β , ρ , I_0 , and $q = 1/\tau$. Since it was announced at a news conference by the mayor of Wuhan on January 23 that 5 million people have left the city by that date, we set the total population $N = S + I + R$ in Wuhan on January 21 to the conservative estimate of 6 million.

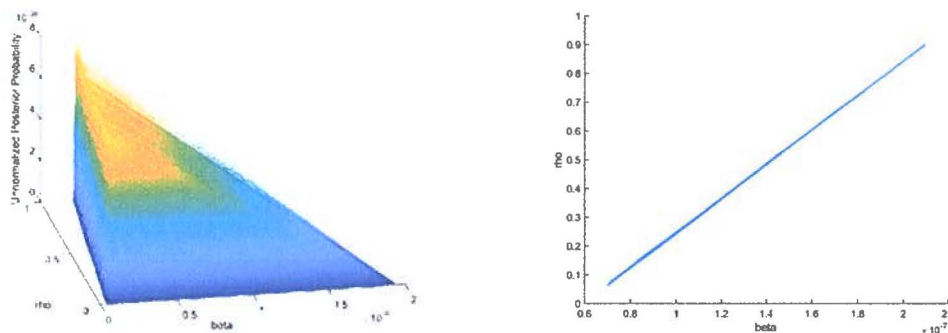
We used the same uniform distributions over the initial range of parameters as the priors for both models, as given in Tables 1 and 2. The affine invariant ensemble Markov chain Monte Carlo algorithm was used to produce posterior distributions for all estimated parameters. From these posterior distributions, we obtain the best-fit values and the 95% credible intervals, as given in Table 1 for the SIR model (2) and in Table 2 for the SEIR model (3).

3.3. Comparing SIR and SEIR models

Using the calibration results for both the SIR and SEIR models in Section 3.3, their corrected Akaike Information Criterion AIC_c are calculated as 174 and 186, respectively. The difference $\Delta = 186 - 174 = 12$ is sufficiently large and this implies that using the SEIR model (3) will produce a significant loss of information in comparison to using the SIR model (2). Accordingly, our further investigation will be carried out using the SIR model (2).

4. Nonidentifiability: linkage between transmission rate β and diagnosis rate ρ

Based on our calibration results of the SIR model in Section 3.3, we detected a linkage between the transmission rate β and the diagnosis rate ρ . In Fig. 2 (a), we show the projection of the unnormalized posterior distribution in the β - ρ parameter



(a) Unnormalized posterior distribution over β - ρ space

(b) A curve of most likely parameters

Fig. 2. Linkage between transmission rate β and diagnosis rate ρ .

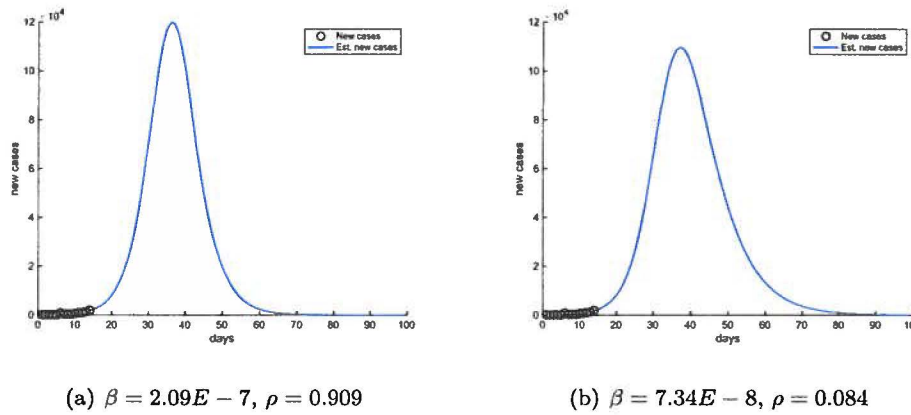


Fig. 3. Model projections using two likely β - ρ combinations, corresponding to two endpoints on the curve in Fig. 2 (b). Day 0 is January 21, 2020.

space. It shows that the largest probability are concentrated along a flat strip rather than on a single point. Correspondingly, as shown in Fig. 2 (b), a curve in the β - ρ parameter space can be determined such that every point on the curve has approximately the same large probability. The linkage between two or more parameters implies the following: (1) the best-fit parameter values are effectively not unique; and (2) there is a continuum of parameter values that cause the model to fit the data approximately equally as well. This phenomenon is often referred to as *nonidentifiability* in the modeling literature.

To further illustrate the significant impact of nonidentifiability on model predictions, we choose two endpoints on the curve in Fig. 2 (b), with respective values $(\beta, \rho) = (2.09e-7, 0.909)$ and $(\beta, \rho) = (7.34e-8, 0.084)$, and we plotted the corresponding projected new cases in Fig. 3(a) and (b), respectively. Fig. 3 shows that the peak height, as well as the duration and scale of the epidemic are different in the two projections, even though both choices of parameter values are effectively equally likely to produce the best fit between the model outcomes and the data.

A striking feature in Fig. 3 is that the peak time of the two different projections are almost identical. This illustrates that, unlike the peak value, the peak time of the epidemic is insensitive to small parameter changes. This important property of the peak time will also be observed in later sections.

We further note that the diagnosis rate ρ is the case-infection ratio that is used to discount of the number of infected individuals $I(t)$ to properly predict the newly confirmed cases. The linkage between β and ρ reflects the dependency of the transmission rate and the case-infection ratio, and hence the scale of the epidemic. We believe that this nonidentifiability is the reason for the wide variability in published model predictions of COVID-19 epidemic.

To reduce the impact of nonidentifiability in model calibration from data, one approach is to search for more independent data, including clinical, surveillance, or administrative data, and from published literature, that can be used for model calibration. This approach is often difficult when facing an outbreak of unknown pathogens that occur in real time such as SARS in 2003 and the current COVID-19. Another approach is to adopt better inference methods and model fitting algorithms to narrow down the otherwise large confidence or credible intervals. Our fitting procedure using Bayesian inference and the affine invariant ensemble Markov chain Monte Carlo algorithm was able to achieve this objective.

5. Baseline predictions for Wuhan and three scenarios

Our baseline predictions for Wuhan are prediction intervals produced by randomly sampling the posterior distribution. The best-fit parameter values and credible intervals are shown in Table 1. The Bayesian inference used the newly confirmed cases for Wuhan contained in the official reports from January 21 to February 4, 2020. This is the period during the lockdown and travel restrictions in Wuhan, but before the further control measures that were undertaken in Wuhan after February 7, 2020, including the drastic increase in the available hospital beds and the door-to-door visits used to identify and quarantine suspected cases. These projections show our estimation for the hypothetical epidemic in Wuhan if further control measures after February 7 were not implemented.

In Fig. 4(a) and (b), we show the distributions of the projected peak time and the estimated values of the control reproduction number \mathcal{R}_c . In Fig. 4(c), we show the projected time course of newly confirmed cases in Wuhan together with its 95% prediction interval. The fit of our model predictions and the newly-confirmed case data is shown for the period between January 21 to February 4 in Fig. 4(d). Based on these projections, if the more restrictive control measures after February 7 in the city were not implemented, the most likely peak time would have occurred on February 27, 2020, with the 95% credible interval from February 23 - March 6. The median value of \mathcal{R}_c is 1.629 with the first quantile 1.414 and the third quantile 1.979. By our projection, without the strict quarantine measures after February 7, the peak case total would reach approximately 120,000, and the epidemic in Wuhan would not be over before mid-May of 2020.

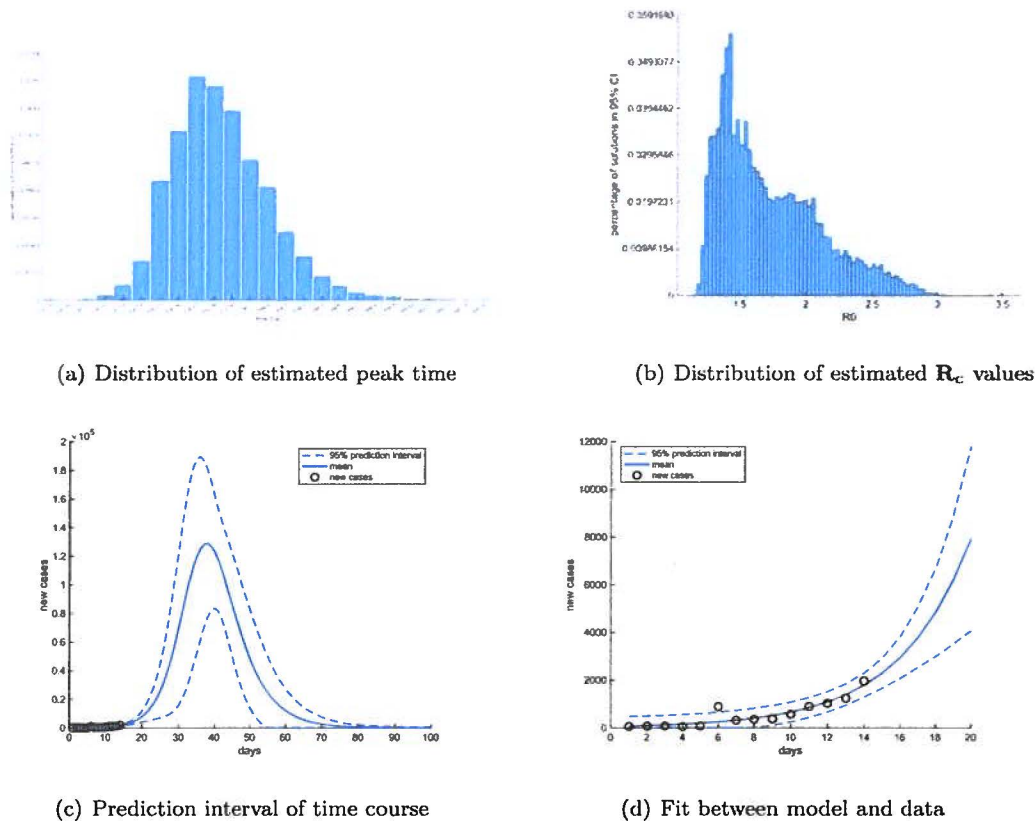


Fig. 4. Distributions of estimated peak time (a) and control reproduction number R_c (b) for COVID-19 epidemic in Wuhan after lockdown. The dashed lines represent the 95% prediction intervals for the time course of COVID-19 epidemic in Wuhan after lockdown (c) and (d). Day 0 in simulations is set at January 21, 2020.

At the time of this manuscript, the consensus among medical experts is that the basic reproduction number R_0 near the beginning of the COVID-19 outbreak in Wuhan is around 2. Our result in Fig. 4 (b) is comparable with earlier estimates and the current consensus. It also shows that, even without the more restrictive control measures in Wuhan undertaken after February 7, the lockdown and travel restrictions in the city had slowed down the transmission and reduced the basic reproduction number to a control reproduction number R_c with a mean value 1.629. We will estimate the impact of the more restrictive control measures in Section 6.

The baseline prediction intervals are computed over a large credible interval of the diagnosis rate ρ , (0.0637, 0.909), which represents a wide range of assumptions on the case-infection ratio and the scale of the epidemic in Wuhan. We further restricted the parameter ρ to three narrower ranges: (0.02, 0.03), (0.05, 0.1), and (0.2, 1), and recalibrated the SIR model (2) with each of the ρ ranges. The resulting predictions for newly confirmed cases are shown in Fig. 5.

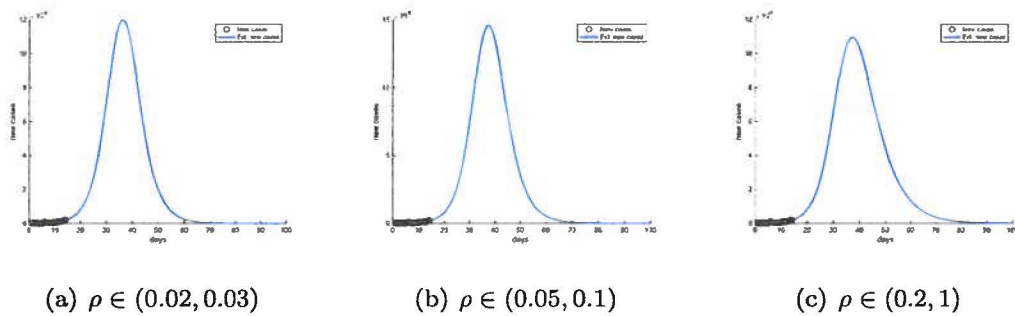


Fig. 5. Model predictions of time courses of COVID-19 epidemic in Wuhan with three different ranges of diagnosis rate ρ : (0.02, 0.03), (0.05, 0.1), and (0.2, 1). Day 0 in the simulations is set at January 21, 2020.

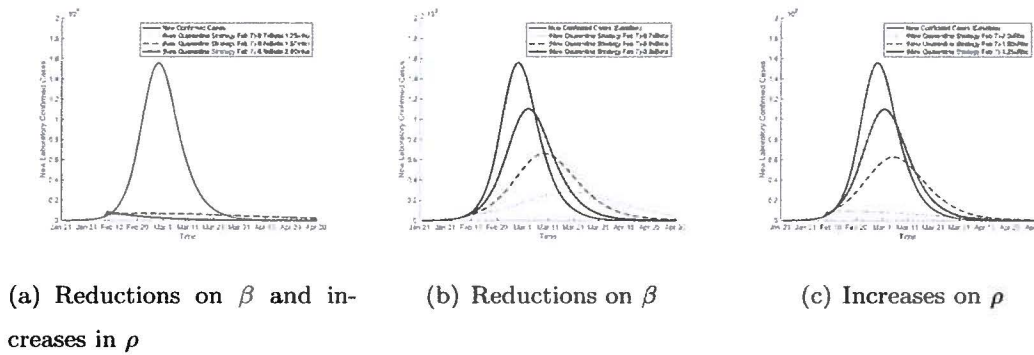


Fig. 6. Predictions of the COVID-19 epidemic in Wuhan with more strict quarantine measures after February 7, 2020. Impacts of reductions in transmission rate β and increases in diagnosis rate ρ are shown in (a). Impacts of only reducing the transmission rate (b) or only increasing the diagnosis rate (c) are also shown for comparison purposes.

In Fig. 5, different ρ ranges have resulted in significant variations in the peak value of cases and the duration of the epidemic. In contrast, the projected peak times are very similar in all three cases, which further demonstrates that the peak time is insensitive to changes in parameters.

6. Impacts of more strict quarantine measures in Wuhan after February 7

After February 7, 2020, Wuhan implemented more strict quarantine measures that included the following: locking down residential buildings and compounds, strict self quarantine for families, door-to-door inspection for suspected cases, quarantining suspected cases and close contacts in newly established hospitals and other quarantine spaces including vacated hotels and university dormitories. The goal of these measures was to reduce transmissions within family clusters and residential compounds. These measures have a direct impact on two parameters in our SIR model (2): reducing the transmission rate β and increasing the diagnosis rate ρ . It is difficult to estimate the exact impacts on these parameters by these measures. We incorporated several likely scenarios of the effects of these measures by adjusting our baseline estimates of β and ρ and we plotted the resulting time courses in Fig. 6.

In Fig. 6 (a), we see that a combination of a 10% reduction in the transmission rate β and a 90% increase in the diagnosis rate ρ can effectively stop the epidemic in its tracks, force the newly diagnosed cases to decline, and significantly shorten the duration of the epidemic.

7. Potential of a second outbreak in Wuhan after the return-to-work

With newly diagnosed cases on the decline in Wuhan and other cities in China since February 14, an urgent task for the authorities is to decide when to allow people to go back to work. Without lifting the ban on traffic in and out of the city, we tested three hypotheses of allowing people to return to work in Wuhan at three different dates: February 24, March 2, and March 31. As shown in Fig. 7, our results predict a significant second outbreak after the return-to-work day.

8. Conclusions

The COVID-19 epidemics have presented China and many other countries in the world with an unprecedented public health challenge in the modern era, with a significant impact on health and public health systems, human lives and national and world economies. Mathematical modeling is an important tool for estimating and predicting the scale and time course of epidemics, evaluating the effectiveness of public health interventions, and informing public health policies. The focus of our study is to demonstrate the challenges facing modelers in predicting outbreaks of this nature and to provide a partial explanation for the wide variability in earlier model predictions of the COVID-19 epidemic.

Our study focused on the COVID-19 epidemic in Wuhan city, the epicentre of the epidemic, during a less volatile period of the epidemic, after the lock down and quarantine of the city. By comparing standard SIR and SEIR models in predicting the epidemic using the Akaike Information Criterion, we showed that, given the same dataset of confirmed cases, more complex models may not necessarily be more reliable in making predictions due to the larger number of model parameters to be estimated.

Using a simple SIR model and the dataset of newly diagnosed cases in Wuhan for model calibration, we demonstrated that there is a linkage between the transmission rate β and the case-infection ratio ρ , which resulted in a continuum of best-fit parameter values, which can produce significantly different model predictions of the epidemic. This is a hallmark of non-identifiability, and the root cause for variabilities in model predictions. The nonidentifiability should not be interpreted as a shortcoming of transmission models; neither is it caused by the limited number of time points in data. Rather, it is caused by

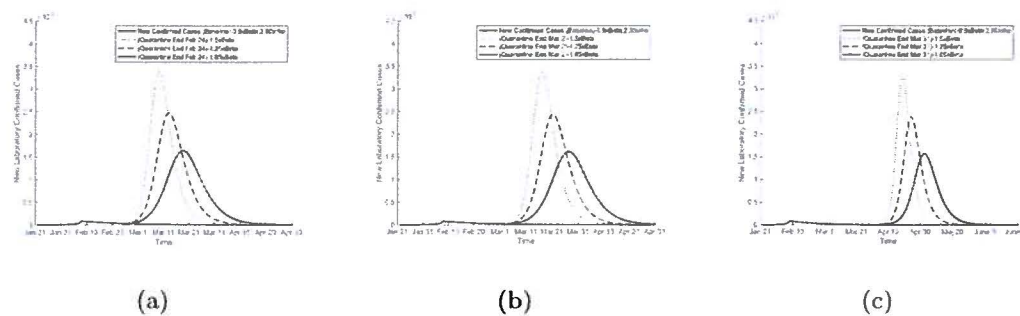


Fig. 7. Model predictions of time courses of COVID-19 epidemic in Wuhan with return to work on (a) February 24, (b) March 2, and (c) March 31, 2020.

the lack of datasets that are independent of the confirmed cases to allow modelers to produce independent estimates of β and ρ . The reliability in model predictions depends on how rigorously the nonidentifiability is addressed in model calibration and on the choice of parameter values.

We demonstrated that Bayesian inference and an improved Markov chain Monte Carlo algorithm, the affine invariant ensemble Markov chain Monte Carlo algorithm, can significantly reduce the wide parameter ranges in the uniform prior and produce workable credible intervals, even in the presence of nonidentifiability. We showed that the estimated credible intervals for the parameters are sufficiently small to allow our credible interval for the peak time to fall within a week. We have further demonstrated that the peak time of the epidemic is much less sensitive to parameter variations than the peak values and the scale of the epidemic. This was also observed in our previous work on predicting seasonal influenza for the Province of Alberta.

We estimated the impact of the Wuhan lockdown and traffic restrictions in the city after January 23 and before February 6, 2020. We show that if the more restrictive control and prevention measures were not implemented in the city, the epidemic would peak between the end of February and first week of March of 2020. Our results can be used to inform public health authorities on what may happen if the more strict quarantine measures after February 7 were not taken.

When the more restrictive measures are incorporated into our model, including the lock down of residential buildings and compounds, the door-to-door search of suspected cases, and the quarantine of suspected cases and their close contacts in newly established hospitals and quarantine spaces, we showed that these measures can effectively stop the otherwise surging epidemic in its tracks and significantly reduce the duration of the epidemic. These findings provide a theoretical verification of the effectiveness of these measures.

We further considered the impact of the return-to-work order on different dates in February and March on the course of the outbreak. Our results show that a second peak in Wuhan is very likely even if the return-to-work happens near the end of March 2020. This may serve as a warning to the public health authorities.

Declaration of competing interest

The authors claim no conflict of interests.

Acknowledgements

Research of MYL is supported in part by the Natural Science and Engineering Research Council (NSERC) of Canada and Canada Foundation for Innovation (CFI).

References

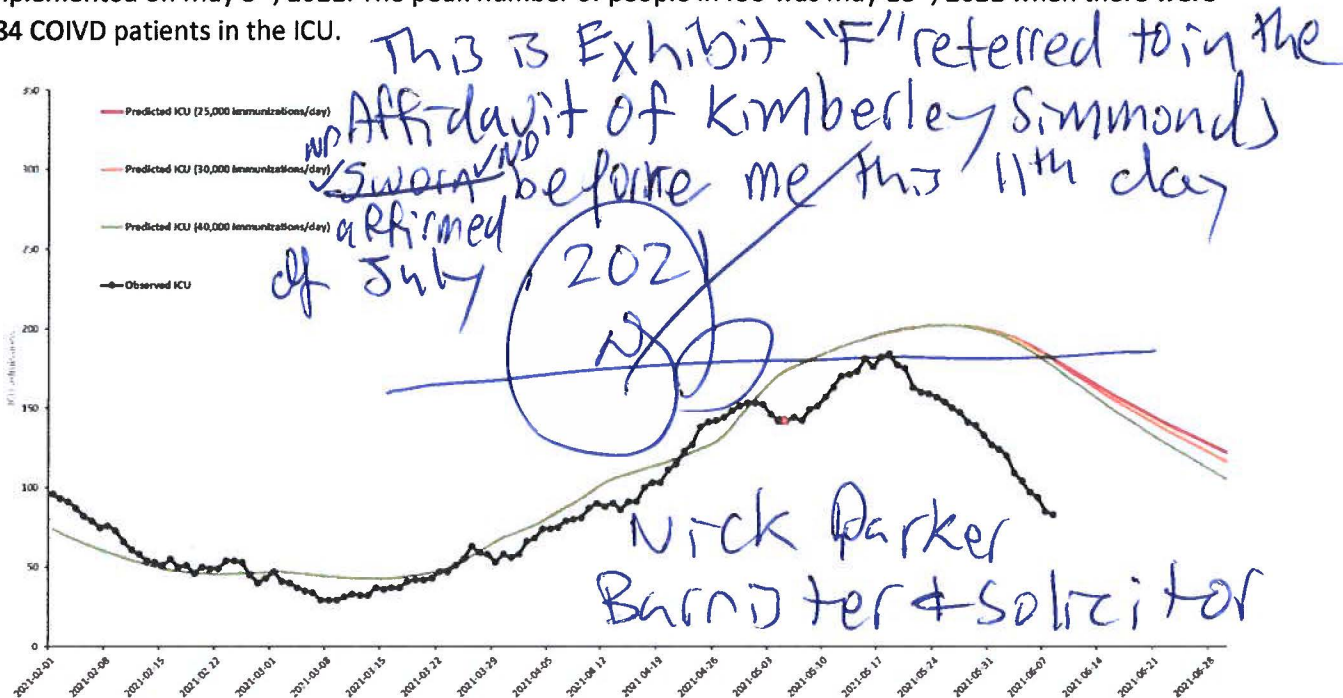
- Akaike, H. (1973). Information theory and an extension of the maximum likelihood principle. In *Second international symposium on information theory* (pp. 267–281). Budapest: Akademiai Kiado.
- Bai, Y., Yao, L., Wei, T., et al. (2020). Presumed asymptomatic carrier transmission of COVID-19. *Journal of the American Medical Association*. <https://doi.org/10.1001/jama.2020.2565>. Published online February 21, 2020.
- Burnham, K., & Anderson, D. (2002). *Model selection and multimodel inference: A practical information-theoretic approach*. New York: Springer-Verlag.
- Chen, M., Shao, Q., & Ibrahim, J. (2000). *Monte Carlo methods in bayesian computation*. New York: Springer-Verlag.
- Chowell, G., Castillo-Chavez, C., Fenimore, P., Kribs-Zaleta, C., et al. (2004). Model parameters and outbreak control for SARS. *Emerging Infectious Diseases*, *10*, 1258–1263.
- Cyranoski, D. (2020). When will the coronavirus outbreak peak? *Nature*. URL <https://www.nature.com/articles/d41586-020-00361-5>.
- Goodman, J., & Weare, J. (2010). Ensemble samplers with affine invariance. *Communications in Applied Mathematics and Computational Science*, *5*, 65–80.
- Gumel, A., Ruan, S., Day, T., et al. (2004). Modelling strategies for controlling SARS outbreaks. *Proceedings of the Royal Society of London B*, *271*, 2223–2232.
- Imai, N., Dorigatti, I., Cori, A., Riley, S., & Ferguson, N. M. (2020). Report 1: Estimating the potential total number of novel coronavirus (2019-nCoV) cases in Wuhan City, China. URL <https://www.imperial.ac.uk/mrc-global-infectious-disease-analysis/news-wuhan-coronavirus/> accessed on February 21, 2020.
- Johnson, J., & Omland, K. (2015). Model selection in ecology and evolution. *Trends in Ecology & Evolution*, *19*, 101–108.
- Kalbfleisch, J. (1979). *Probability and statistical inference*. New York: Springer-Verlag.

- Lintusaari, J., Gutmann, M., Kaski, S., & Corander, J. (2016). On the identifiability of transmission dynamic models for infectious diseases. *Genetics*, *202*, 911–918. <https://doi.org/10.1534/genetics.115.180034>.
- Lipsitch, M., Cohen, T., Cooper, B., Robins, J., et al. (2003). Transmission dynamics and control of severe acute respiratory syndrome. *Science*, *300*, 1666–1670.
- Lynch, S. (2007). *Introduction to applied bayesian statistics and estimation for social scientists*. New York: Springer.
- May, W. (2015). A parallel implementation of MCMC. URL: [www.semanticscholar.org/paper/A-parallel-implementation-of-MCMC-May/695d03ebf49cb222e0476de82e101893ff98992d?utm&dollar_\protect\unhbox\voidb&x\hbox\[source\]=$email](http://www.semanticscholar.org/paper/A-parallel-implementation-of-MCMC-May/695d03ebf49cb222e0476de82e101893ff98992d?utm&dollar_\protect\unhbox\voidb&x\hbox[source]=$email) available at Semantic Scholar.
- National Health Commission of the People's Republic of China. (2020). Daily briefing on novel coronavirus cases in China. URL www.nhc.gov.cn/ accessed on February 21, 2020.
- Portet, S. (2020). A primer on model selection using the Akaike information criterion. *Infectious Disease Modelling*, *5*. <https://doi.org/10.1016/j.idm.2019.12.010>.
- Raue, A., Kreutz, C., Maiwald, T., Bachmann, J., et al. (2009). Structural and practical identifiability analysis of partially observed dynamical models by exploiting the profile likelihood. *Bioinformatics*, *25*, 1923–1929. <https://doi.org/10.1093/bioinformatics/btp358>.
- Read, J., Bridgen, J., Cummings, D., Ho, A., & Jewell, C. (2020). Novel coronavirus 2019-nCoV: Early estimation of epidemiological parameters and epidemic predictions. <https://doi.org/10.1136/adc.2006.098996>. available at medRxiv.
- Roda, W. (2020). Bayesian inference for dynamical systems. *Infectious Disease Modelling*, *5*. <https://doi.org/10.1016/j.idm.2019.12.007>.
- Rossi, R. (2018). *Mathematical statistics: An introduction to likelihood based inference*. New York: John Wiley & Sons.
- Shen, M., Peng, Z., Xiao, Y., & Zhang, L. (2020). Modelling the epidemic trend of the 2019 novel coronavirus outbreak in China. <https://doi.org/10.1101/2020.01.23.916726>. available at bioRxiv.
- Sugiura, N. (1978). Further analysis of the data by Akaike's information criterion and the finite corrections. *Communications in Statistics - Theory and Methods*, *7*, 13–26. <https://doi.org/10.1080/03610927808827599>.
- Tang, B., Bragazzi, N., Li, Q., Tang, S., Xiao, Y., & Wu, J. (2020a). An updated estimation of the risk of transmission of the novel coronavirus (2019-nCoV). *Infectious Disease Modelling*, *5*, 248–255. <https://doi.org/10.1016/j.idm.2020.02.001>.
- Tang, B., Wang, X., Li, Q., Bragazzi, N., T. S., Xiao, Y., et al. (2020b). Estimation of the transmission risk of 2019-nCoV and its implication for public health interventions. *Journal of Clinical Medicine*, *9*, 462.
- US, C. D. C. (2020). Weekly US influenza surveillance report. URL <https://www.cdc.gov/flu/weekly/index.htm> accessed on February 21, 2020.
- van der Vaart, A. (1998). *Asymptotic statistics*. Cambridge University Press.
- WHO. (2003). Consensus document on the epidemiology of severe acute respiratory syndrome (SARS). URL: <https://www.who.int/csr/sars/en/WHOconsensus.pdf> accessed on February 21, 2020.
- WHO. (2020). Statement on the second meeting of the International Health Regulations (2005) Emergency Committee regarding the outbreak of novel coronavirus (2019-ncov). URL [https://www.who.int/news-room/detail/30-01-2020-statement-on-the-second-meeting-of-the-international-health-regulations-\(2005\)-emergency-committee-regarding-the-outbreak-of-novel-coronavirus-\(2019-ncov\)](https://www.who.int/news-room/detail/30-01-2020-statement-on-the-second-meeting-of-the-international-health-regulations-(2005)-emergency-committee-regarding-the-outbreak-of-novel-coronavirus-(2019-ncov)) accessed on February 21, 2020.
- Wu, J., Leung, K., & Leung, G. (2020). Nowcasting and forecasting the potential domestic and international spread of the 2019-nCoV outbreak originating in Wuhan, China: A modelling study. *The Lancet*, *395*, 689–697. [https://doi.org/10.1016/S0140-6736\(20\)30260-9](https://doi.org/10.1016/S0140-6736(20)30260-9). URL <http://www.sciencedirect.com/science/article/pii/S0140673620302609>.
- You, C., Deng, Y., Hu, W., Sun, J., Lin, Q., et al. (2020). Estimation of the time-varying reproduction number of COVID-19 outbreak in China. <https://doi.org/10.1101/2020.02.08.20021253>. available at medRxiv.
- Yu, X. (2020). Updated estimating infected population of Wuhan coronavirus in different policy scenarios by SIR model. URL <http://uni-goettingen.de/en/infectious+diseases/619691.html> (2020) accessed on February 22, 2020.
- Zhang, J., Lou, J., Ma, Z., et al. (2005). A compartmental model for the analysis of SARS transmission patterns and outbreak control measures in China. *Applied Mathematics and Computation*, *162*, 909–924.
- Zhao, S., Musa, S., Lin, Q., Ran, J., Yang, G., et al. (2020). Estimating the unreported number of novel coronavirus (2019-nCoV) cases in China in the first half of January 2020: A data-driven modelling analysis of the early outbreak. *Journal of Clinical Medicine*, *9*, 388.

COVID-19 – Modelling Predictions

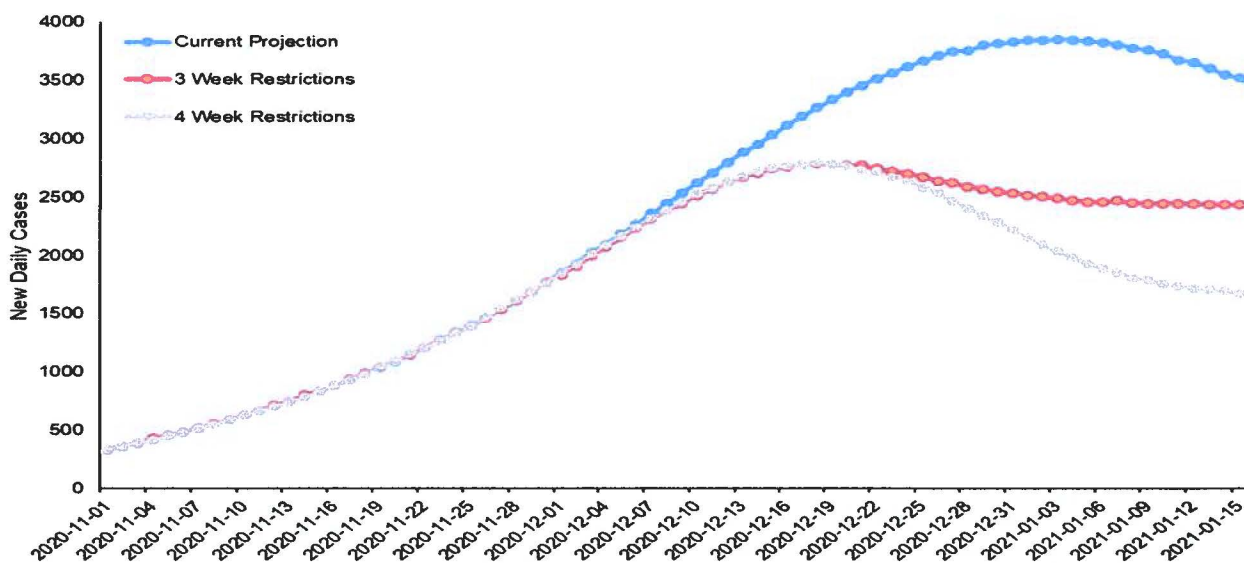
Spring 2021 Projections

In the following graph predicted the impact of a third wave on ICU admissions without restrictions implemented on May 5th, 2021. The peak number of people in ICU was May 18th, 2021 when there were 184 COVID patients in the ICU.



Fall 2020 Projections

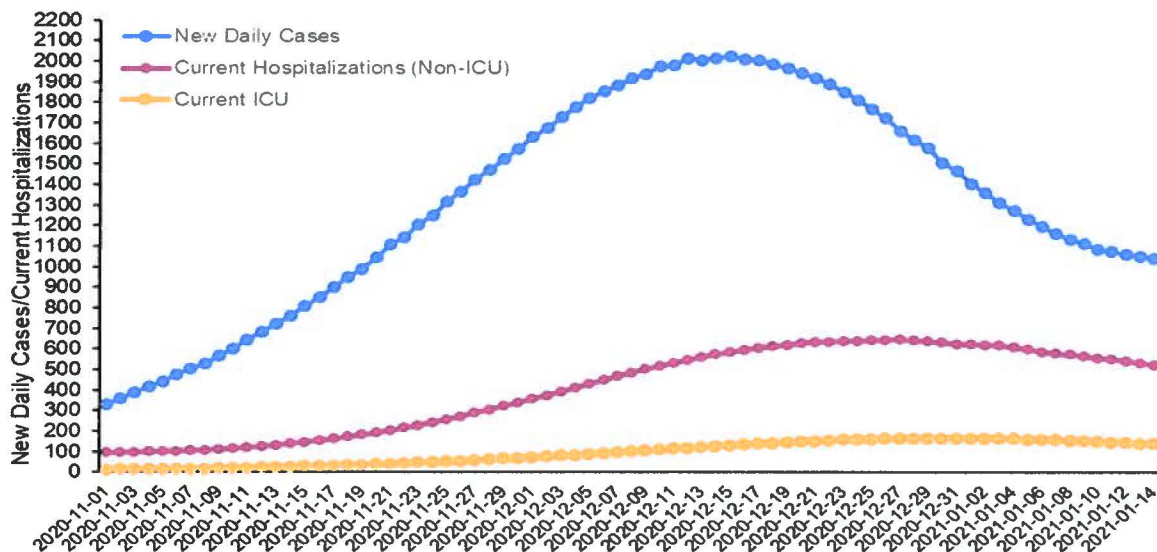
The following graph predicted the impact of restrictions implement November 24th and varying the duration of the restrictions, using data up to October 1, 2020.



1/2

COVID-19 – Modelling Predictions

The revised estimates were based on additional simulations and data up to October 31, 2020. The estimated peak for cases was December 15, 2020 with 2,023 cases and the actual was December 13, 2020 with 1,875. The hospitalizations due to COVID were estimated to peak at 648 on December 27, 2020 in fact the peak was December 30, 2020 with 905 hospitalizations. Some of the difference in actual and predicted hospitalizations were due to the outbreaks in acute care. COVID related ICU were estimated to peak at 168 on December 29, 2020 and the peak was December 28, 2020 with 154 patients in the ICU.



Spring 2020 Projections

Please see <https://www.alberta.ca/assets/documents/covid-19-case-modelling-projection.pdf>
<https://www.alberta.ca/assets/documents/covid-19-case-modelling-projection-april-28.pdf>

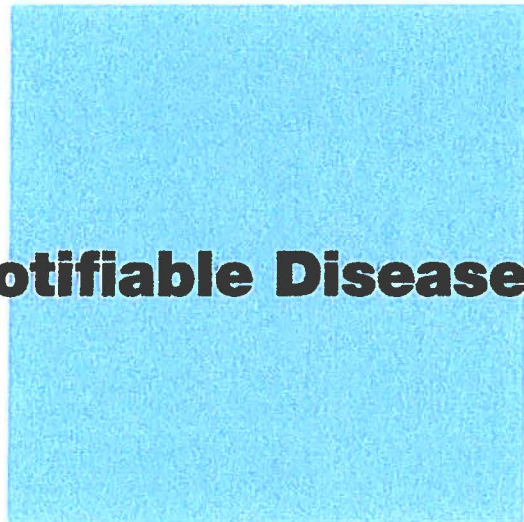
This is Exhibit G referred to in the Affidavit of Kimberley Simmonds

Kimberley

Sworn before me this 11th day of July A.D., 2021

A Notary Public, A Commissioner for Oaths
in and for the Province of Alberta

Nick Parker
Barrister & Solicitor



Alberta Notifiable Disease Incidence

A Historical Record
1919-2014

Acknowledgements

Prepared by Rosa Maheden
Business Analyst

Contributions Kimberley Simmonds
Manager, Infectious Disease, EPI
Theresa Lohman
Manager, Communicable Disease
Larry Svenson
Director, Epidemiology Surveillance

Statistical support Michael Sanderson
Manager, Monitoring

This document was prepared under the guidance of Health System Accountability and Performance Division with review from senior staff of Surveillance and Assessment Branch and the Office of the Chief Medical Officer of Health.

ISBN 978-1-4601-2560-1 (Print)

ISBN 978-1-4601-2561-8 (PDF)

Table of Contents

Executive Summary	2
Introduction	3
Dedication	4
Selected Notifiable Communicable Diseases	5
Campylobacteriosis.....	6
Chlamydial Infections	6
Diphtheria	7
Hemorrhagic Colitis (E. coli O157:H7).....	7
Giardiasis.....	8
Gonococcal Infections	8
<i>Haemophilus Influenzae</i> Invasive, Type B	9
Hepatitis A.....	9
Hepatitis B.....	10
Hepatitis C.....	10
Human Immunodeficiency Virus (HIV) Infection	11
Measles	11
Meningococcal Disease, Invasive	12
Mumps	12
Pertussis.....	13
Pneumococcal Disease, Invasive.....	13
Poliomyelitis	14
Rubella	14
Salmonellosis	15
Smallpox.....	15
Syphilis	16
Tuberculosis	16
Typhoid and Paratyphoid	17
Data Tables.....	19

Executive Summary

The success of public health measures, implemented over the past century, have greatly contributed to the decrease of communicable disease incidence in Alberta. Highly effective immunization programs and treatments have virtually eliminated communicable diseases such as measles, diphtheria and polio, while smallpox has been completely eradicated. Measures instituted to improve the quality of food, water, and sanitation have contributed to a marked decrease in enteric diseases such as giardiasis and typhoid.

Despite the drop in communicable disease incidence as a whole, the occurrence of some diseases such as sexually transmitted infections (STI's), are on the rise. Increases in international travel, coupled with new emerging pathogens, such as SARS and West Nile virus, highlight the importance of continued surveillance and constant preparation to detect and respond to new, emerging and re-emerging communicable disease threats.

Introduction

Diseases that are notifiable in Alberta are defined in the *Public Health Act, Communicable Diseases Regulation* for the province and must be reported to the Office of the Chief Medical Officer of Health (OCMOH). These diseases are notifiable because they have one or more of the following characteristics:

- they cause serious illness,
- they have the potential to infect many people or
- they can be controlled or prevented by appropriate interventions.

There are several categories of notifiable diseases:

- enteric illnesses,
- vaccine preventable diseases,
- sexually transmitted infections,
- blood-borne pathogens,
- respiratory illnesses,
- syndromic illnesses,
- environmental and zoonotic illnesses.

This report links the various roles of the Health System Accountability and Performance Division by providing a historical account of selected notifiable communicable diseases in Alberta and identifying trends in incidence, thus allowing public health professionals to formulate a plan for future disease prevention. Selected communicable diseases illustrated on the following pages highlight areas where public health measures have succeeded in decreasing disease incidence, while also identifying other diseases that still remain a challenge. The data tables included in the document provide disease incidence and rate per year from 1919 to 2014 as it was collected.

Dedication



Dr. John Waters (1943 – 2001)

This report is dedicated to the late Dr. John Waters.

Dr. Waters was a highly respected Chief Medical Officer of Health in Alberta for 21 years. He was a passionate public health advocate and leader in protecting the health of Albertans, in particular children. His main focus was controlling communicable diseases through immunization programs.

Dr. Waters felt strongly about the importance of communicable disease surveillance and the value of historical data. John's collection of notifiable disease data for the province dated back to 1919, which was compiled in various formats. Based on his wisdom and experience, the data in this report is presented in a format that provides the reader with easy access to this important historical data. Lessons learned from the past are applied to the emerging diseases of today.

"Dr. Waters has made the well being of Canadians his life work"

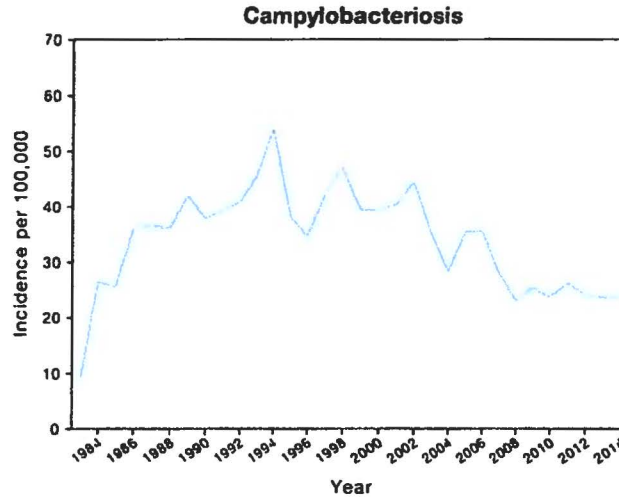
Adrienne Clarkson, Governor General of Canada,
December 1, 2002



Selected Notifiable Communicable Diseases

Campylobacteriosis

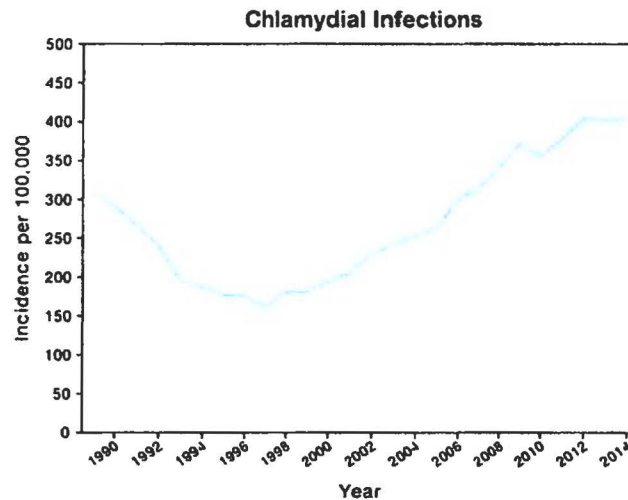
Campylobacteriosis is an enteric illness caused by bacteria in the *Campylobacter* group. The two most common species are *C. jejuni* and *C. coli*.



Campylobacteriosis became reportable in 1983 and is the most commonly reported enteric illness. Reported rates of campylobacteriosis increased between 1983 and 1994 and remained fairly constant until 2003. Since 2004, Alberta has reported between 830 and 1,216 cases each year.

Chlamydial Infections

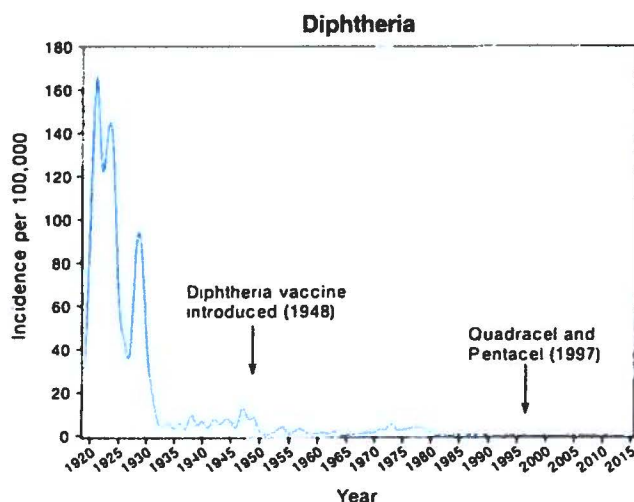
Chlamydia is caused by the bacterium *Chlamydia trachomatis*.



Chlamydia data has been available since 1989. Between 1989 and 1993, reported rates of chlamydial infections decreased and then remained consistent until 1999. Since 2000, Alberta has seen a marked increase in the infection rate rising from 194 cases per 100,000 in 2000 to 403 cases per 100,000 in 2014. Currently, it is the most common bacterial sexually transmitted infection (STI).

Diphtheria

Diphtheria is caused by the bacterium *Corynebacterium diphtheriae*.

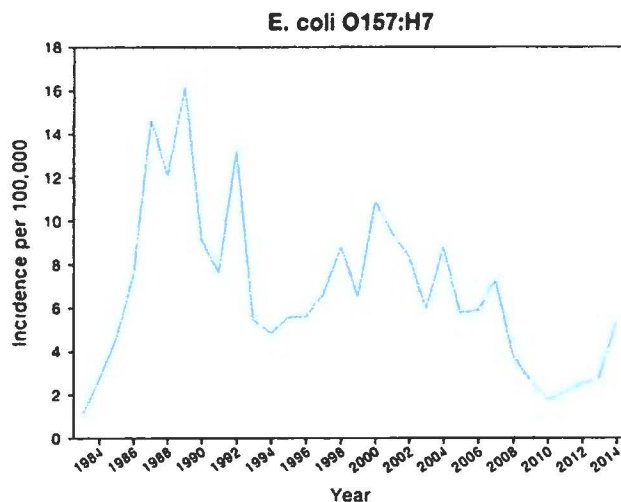


Data has been available since 1919. The highest recorded number of diphtheria cases was in 1921 when 978 cases were reported. Before routine immunization was introduced in 1948 it was one of the most common causes of death in children under five years of age. Since then there has been a substantial decline in morbidity and mortality.

From 1981 to 1994, only one acute respiratory case and 13 acute cutaneous cases were reported. In 2004 and 2007 sporadic cutaneous diphtheria cases were detected.

Hemorrhagic Colitis (E. coli O157:H7)

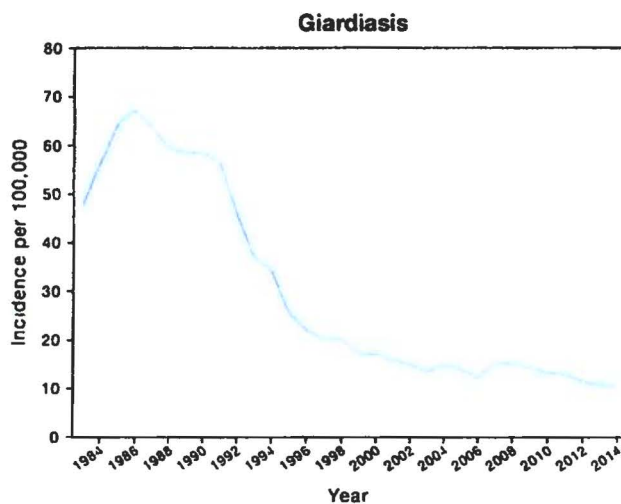
Hemorrhagic colitis is commonly caused by the bacterium *Escherichia coli serotype O157:H7*.



Escherichia coli O157:H7 became reportable in 1983. Rates of *E. coli O157:H7* are highly variable, primarily due to the outbreaks it causes. Since reportability, Alberta has reported between 26 and 405 cases per year.

Giardiasis

Reportable Giardiasis is an intestinal infection caused by the parasite *Giardia lamblia*.

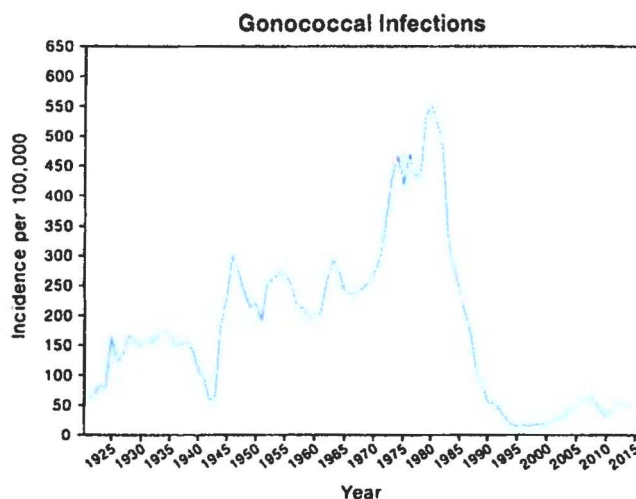


Giardiasis became reportable in 1983. Since 1986 when cases peaked at just over 1,600 incidence of giardiasis has decreased to between 400 and 550 cases per year.

This decreasing trend aligns with the Canadian one.

Gonococcal Infections

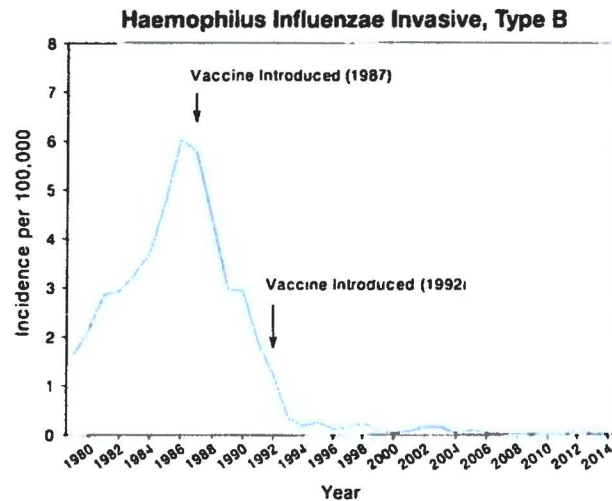
Gonorrhea, the second most common sexually transmitted infection, is caused by the bacterium *Neisseria gonorrhoea*.



Gonococcal disease data has been available since 1919. Between 1980 and 1997, the reported rate of gonococcal infections decreased significantly. This decline has been partially attributed to change in sexual practices due to increased awareness of the threat of HIV/AIDS. Rates began to increase in 1997. Since 2000, Alberta has reported a rate between 19 and 62 cases per 100,000.

Haemophilus Influenzae Invasive, Type B

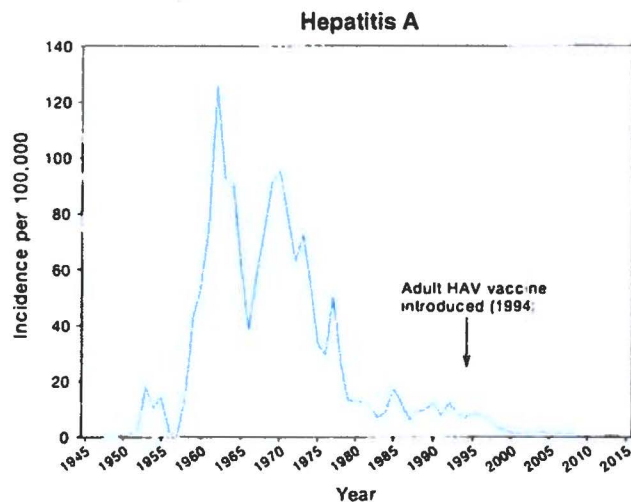
Haemophilus influenzae type B (Hib) bacteria is known to cause bacterial meningitis. Historically, rates were highest in children less than five years of age.



Invasive Hib became reportable in Alberta in 1979. With the introduction of Hib vaccine in 1987, the incidence of infection has dropped significantly. Alberta reported a peak of 147 cases of Hib in 1986 and only sporadic cases since 1993.

Hepatitis A

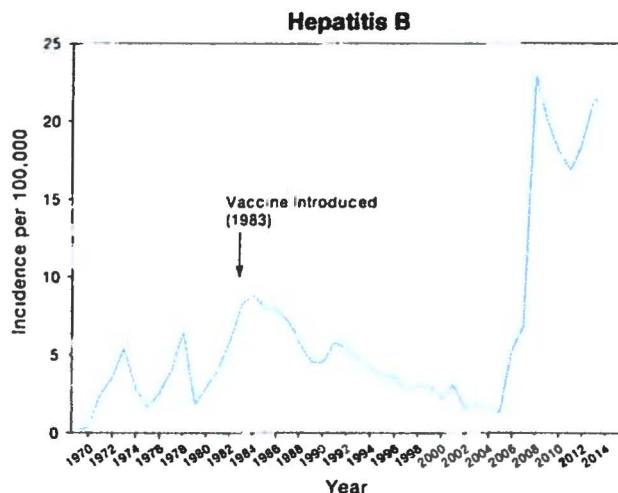
Hepatitis A is an acute viral illness caused by the hepatitis A virus.



With the exception of 1957, hepatitis A data has been available since 1949 although it was not formally reportable until 1969. Reported rates of hepatitis A have been steadily decreasing since 1970. Since 2000, Alberta has reported between 24 and 65 cases annually.

Hepatitis B

Hepatitis B, formally referred to as Serum Hepatitis, is caused by the hepatitis B virus.

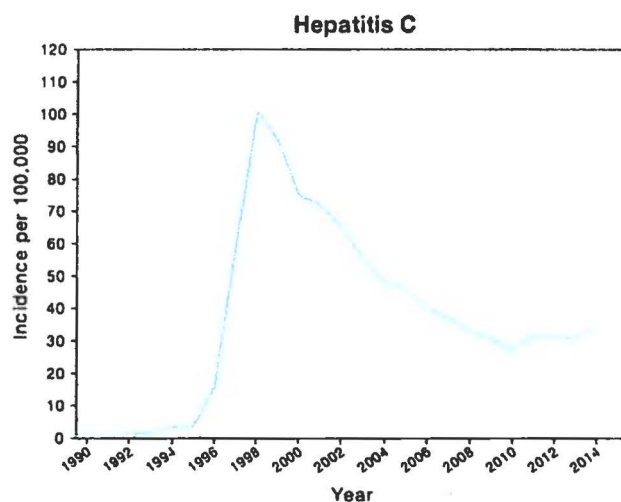


Acute hepatitis B cases became reportable in Alberta in 1969, and chronic cases in 2008. Reported rates of acute hepatitis B infections have been decreasing since 1983. A further reduction was seen once routine immunization programs were introduced in 1995. Since 1995, Alberta has reported between 20 and 100 acute cases each year.

The increase seen in 2006 onward is correlated with screening practices and an increase in new Albertans from countries where Hepatitis B is endemic.

Hepatitis C

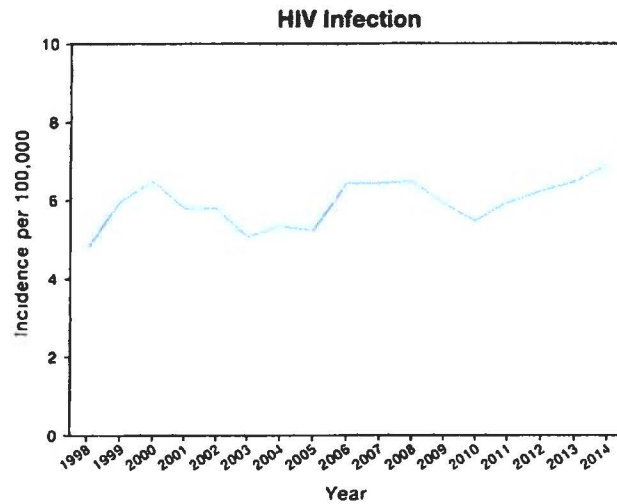
Hepatitis C, a blood-borne pathogen, caused by the hepatitis C virus, became reportable in 1996. Both acute and chronic cases are reportable.



Hepatitis C is one of the most common notifiable diseases in Alberta. In 1998, Alberta reported just in excess of 2,900 cases. Since then, the number of identified hepatitis C cases reported has decreased steadily.

Human Immunodeficiency Virus (HIV) Infection

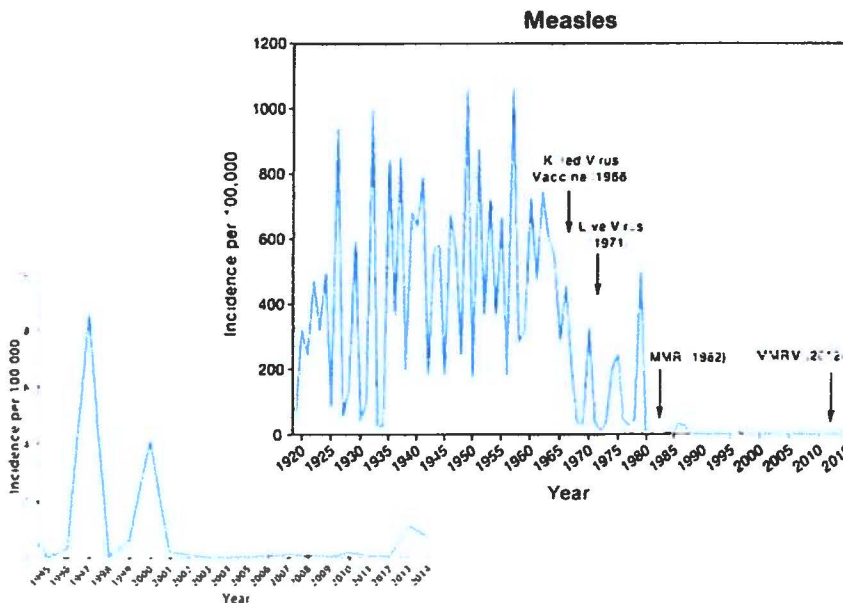
Human Immunodeficiency Virus (HIV) is the virus that causes Acquired Immunodeficiency Syndrome (AIDS).



HIV became reportable in Alberta in May 1998, with reported rates of HIV infections remaining relatively constant. Since 1998, Alberta has reported between 138 and 284 cases per year.

Measles

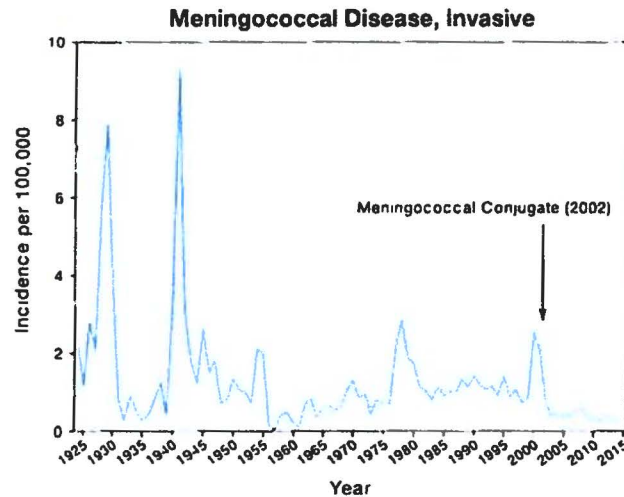
Measles, a highly communicable disease caused by the measles virus in the genus *Morbillivirus*, is one of the most serious diseases of childhood.



Measles data for Alberta has been available since 1919. Historically, outbreaks of measles occurred approximately every three years. The highest recorded number of measles cases was in 1957 when 12,337 cases were reported. Routine immunization has led to a substantial decline in measles morbidity and mortality. Since 2000, measles cases have been sporadic. In 2013 there was a measles outbreak in Southern Alberta with 44 confirmed cases reported.

Meningococcal Disease, Invasive

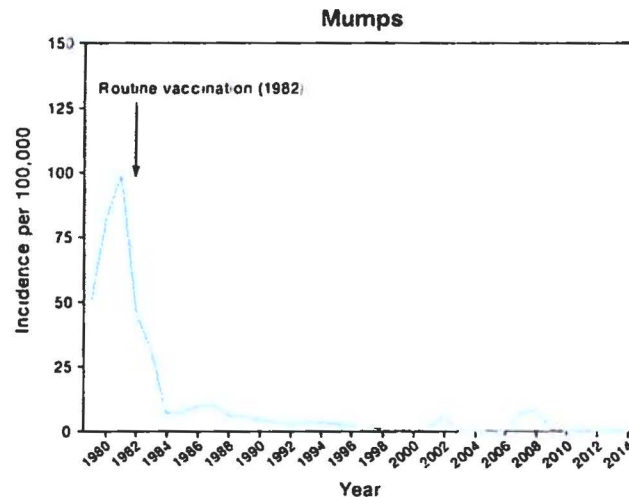
Invasive meningococcal disease (IMD) is caused by the bacteria *Neisseria meningitidis*.



Data on IMD has been available since 1924. Historically, outbreaks occur every ten to twenty years. A significant outbreak recorded in Alberta began in December 1999, involving over 140 cases. In 2002, a routine infant immunization program to prevent serogroup C infection was introduced. Since then less than 25 cases have been reported each year.

Mumps

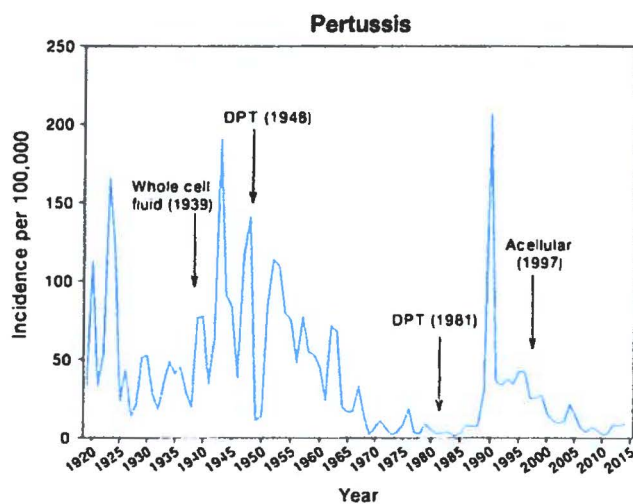
Mumps is caused by a virus that is a member of the *Paramyxoviridae* family.



Mumps became reportable in 1979. The highest number of reported cases occurred in 1981 when 2,217 cases were reported. Routine immunization programs introduced in 1982 have led to a substantial decline in the number of cases of mumps. The last outbreak began in the fall of 2007 in southern Alberta resulting in more than 550 cases.

Pertussis

Pertussis, a bacterial disease caused by the bacterium *Bordetella pertussis*, is a cyclical disease, with outbreaks



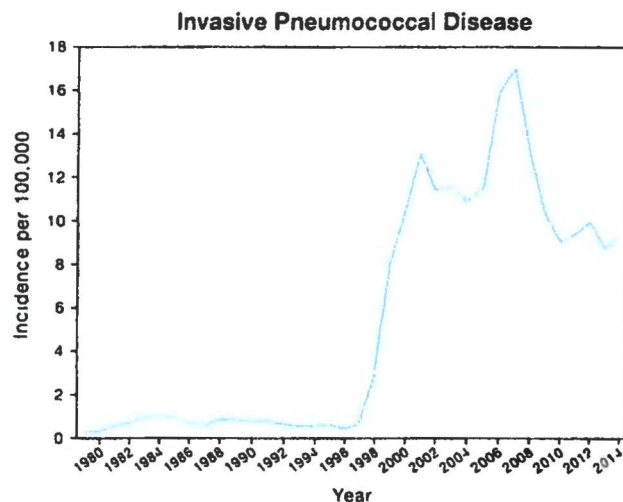
expected approximately every five years among those not immunized.

Pertussis data has been available since 1919. Since the introduction of the diphtheria-pertussis-tetanus vaccine in 1948, the overall rate of pertussis has decreased. A significant outbreak occurred between September 1989 and April 1990 with 2,921 cases reported. In 1997,

the whole cell pertussis vaccine was replaced by the currently used acellular product.

Pneumococcal Disease, Invasive

Pneumococcal disease is caused by the bacterium *Streptococcus pneumoniae*, of which there are approximately 90 serotypes.

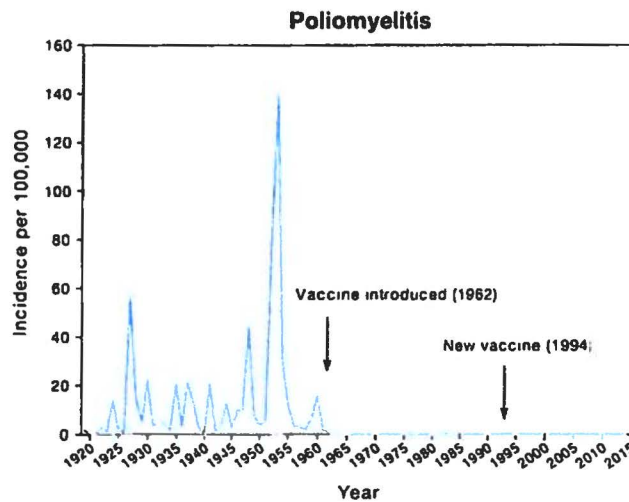


Invasive pneumococcal disease became reportable in 1998. A routine polysaccharide immunization program was introduced in 1997 to high risk persons over the age of two years. Invasive *Streptococcus pneumoniae* was put under surveillance to monitor the success of the enhanced pneumococcal vaccine program. A 7-valent conjugate vaccine was

introduced in 2002 and in 2010 a 13-valent vaccine replaced it. Despite the introduction of these immunization programs, overall rates remain high, although rates among infants have decreased.

Poliomyelitis

Poliomyelitis is caused by *poliovirus types 1, 2 and 3*.



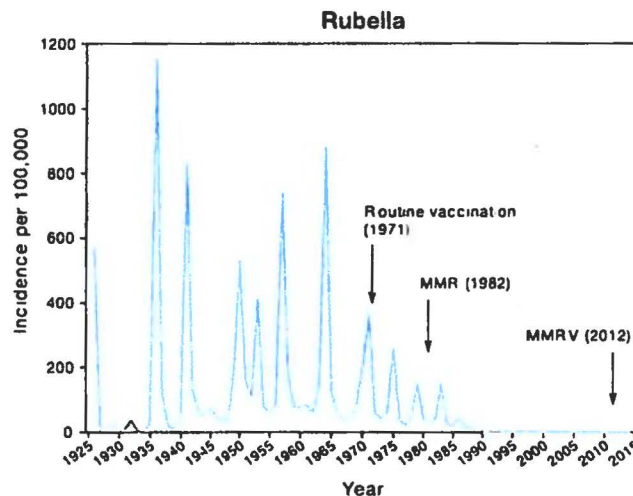
Polio data has been available since 1919. Polio has been a significant source of morbidity and mortality. Immunization against polio has almost eradicated this disease from the Western Hemisphere. Indigenous wild poliovirus cases still occur in parts of Africa and Asia.

Since 1968, three cases of symptomatic polio were reported in Alberta,

with the last case reported in 1979. Two were attributed to the administration of live virus vaccine, and the third was a non-immunized child. Introduction of inactivated polio vaccine in 1956 has eliminated the risk of vaccine associated polio disease.

Rubella

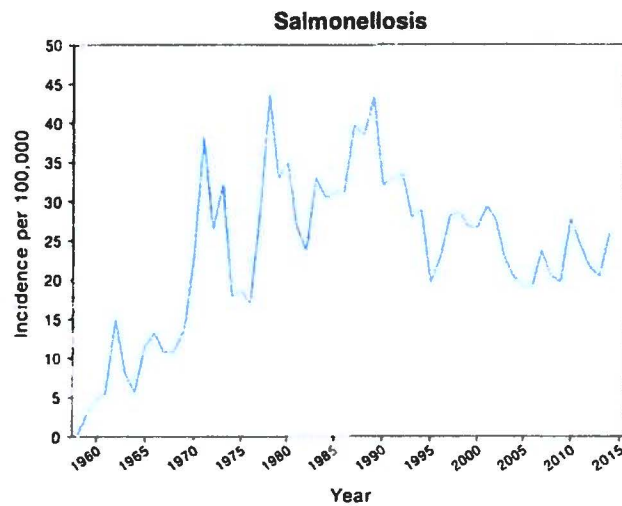
Rubella is caused by the *rubella virus*.



Rubella has been reportable since 1926. Rubella is a cyclical disease, with outbreaks expected approximately every five to seven years in susceptible populations. Routine immunization programs introduced in 1971 contributed to the substantial decline in the number of cases of rubella. Since 2000 only 20 cases of rubella have been reported.

Salmonellosis

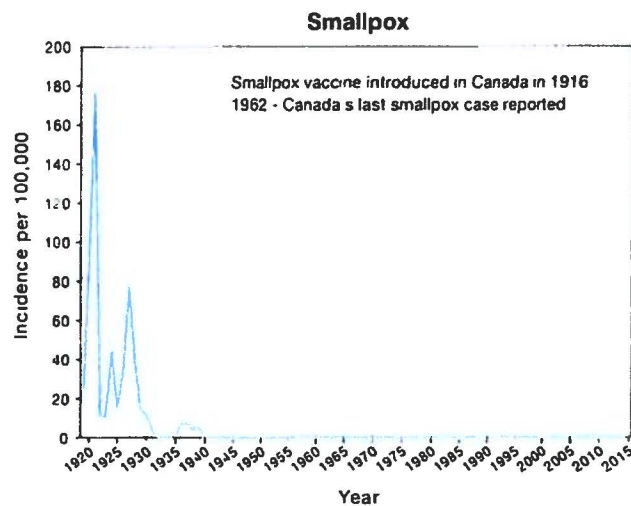
Salmonellosis is caused by *Salmonella* bacteria.



Salmonellosis has been reportable since 1959. Reported rates of salmonellosis are variable, primarily due to the high transmissibility potential of the disease. Since 2004, Alberta has reported rates between 20 and 28 cases per 100,000 each year.

Smallpox

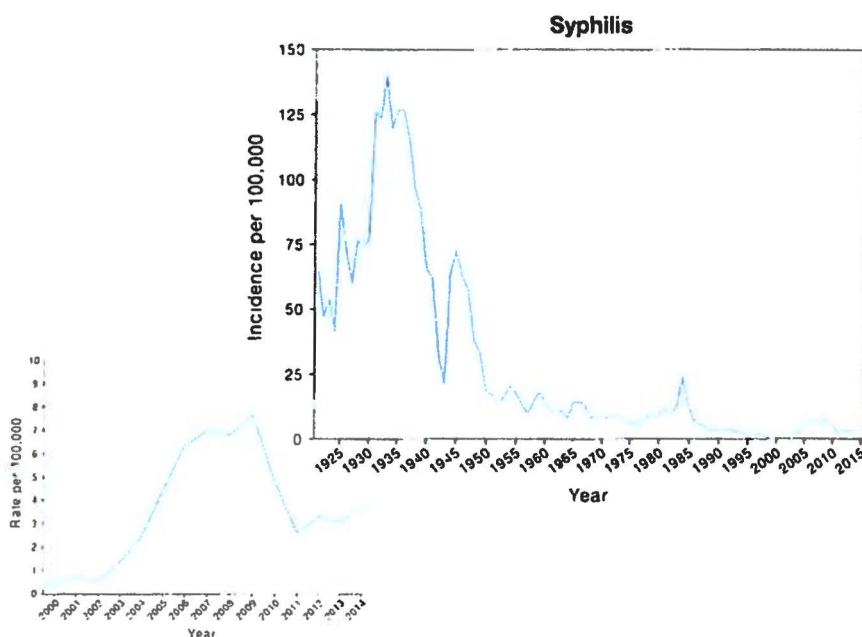
Smallpox is caused by the *Variola virus*. Immunization has eradicated wild smallpox worldwide, as declared in 1978 by the World Health Organization.



Smallpox data is available since 1919. Routine immunization, introduced in 1916, was discontinued in Canada in 1980. The last case of smallpox in Alberta occurred in 1943.

Syphilis

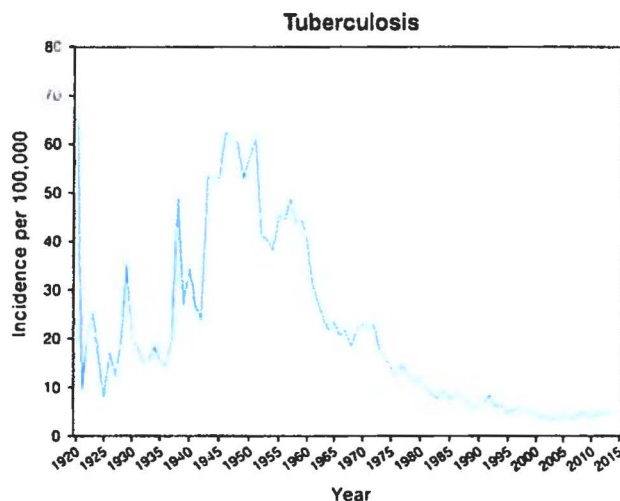
Syphilis is caused by *Treponema pallidum*, a spirochete.



Syphilis data has been available since 1921. Syphilis rates decreased after 1930 with the advent of penicillin. Since then, a significant syphilis outbreak occurred in 1984 with 574 cases reported. Subsequent years showed a decline in the number of cases until 2003 when the number of cases again increased. The rate of cases reported declined in 2010 after the launch of a public awareness campaign.

Tuberculosis

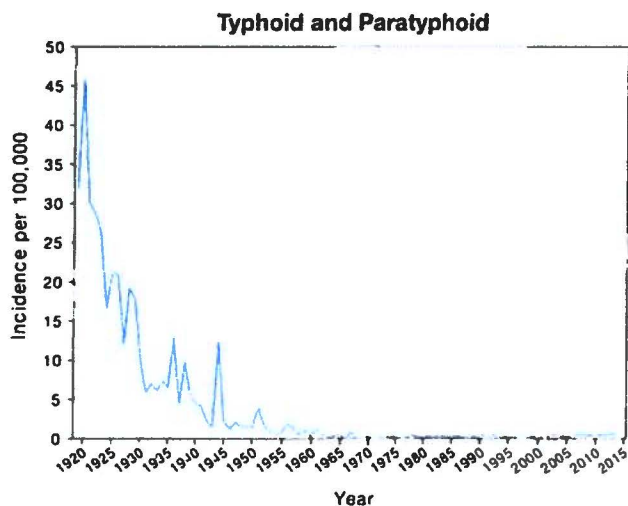
Tuberculosis is caused by the bacteria *Mycobacterium tuberculosis*.



Tuberculosis data has been available since 1920. With the advent of antibiotics and introduction of BCG vaccine in 1956, the number of cases of tuberculosis has decreased until the 80's when rates reached a plateau. Since 2000 fewer than 217 cases are reported each year. In recent years, the majority of tuberculosis cases were amongst foreign born Albertans.

Typhoid and Paratyphoid

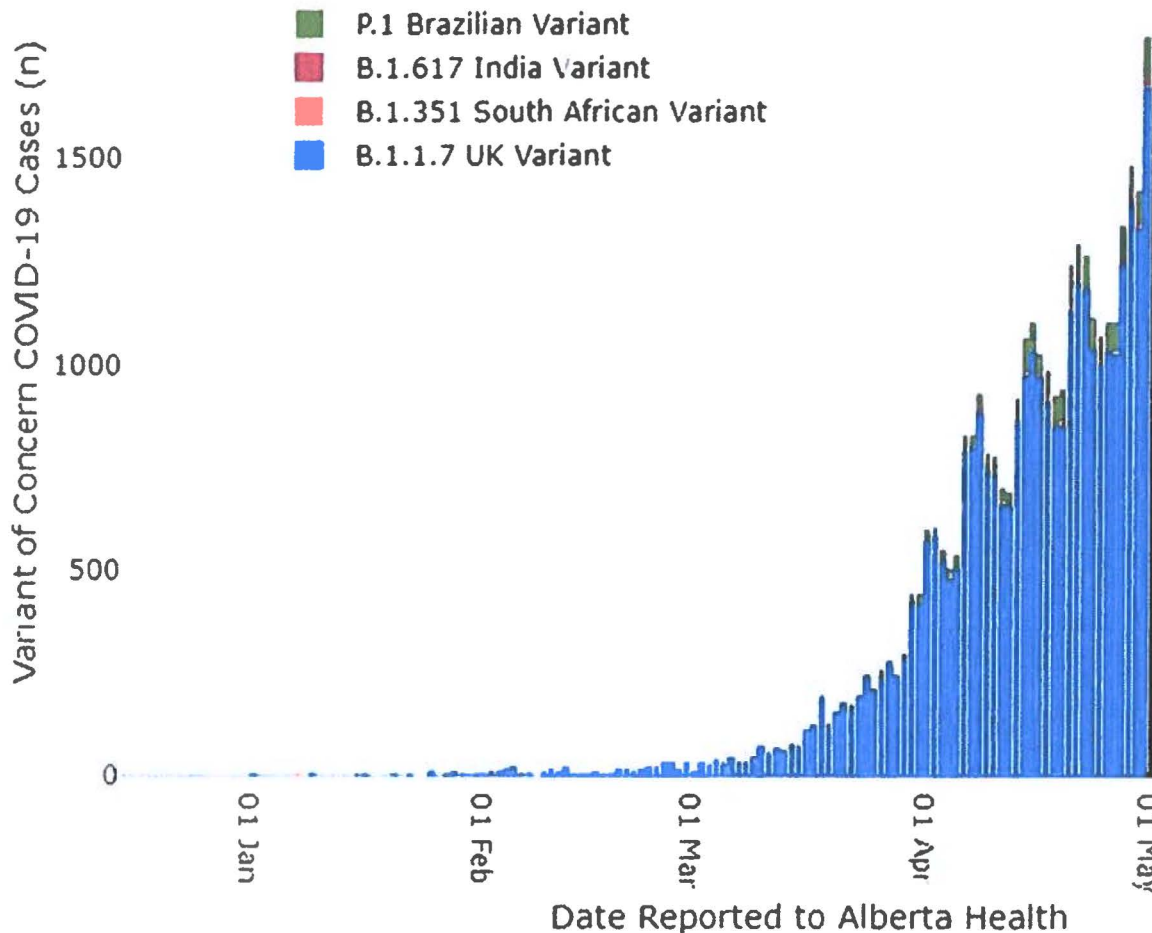
Typhoid and paratyphoid are caused by the bacteria *Salmonella typhi* and *Salmonella paratyphi* respectively. In most cases, typhoid is not a chronic disease, however, a few people remain infected for life.



Typhoid fever data has been available since 1919; paratyphoid since 1929. Reported rates of typhoid fever have been steadily decreasing since the 1920s. Since 2000, recent typhoid and paratyphoid cases in Alberta were almost exclusively associated with foreign travel to an endemic area with the exception of three cases in 2014 where a link to an endemic area could not be found.

COVID-19 – Variants of Concern

The first variant of concern (VOC), the B.1.1.7 variant, was identified in December 25, 2020 from an individual that recently travelled to the UK. By May 1, 2021 a total of 35,291 VOC cases were identified and the B.1.1.7 variant was the dominant strain and more new daily cases are VOCs than the original wild type strain.

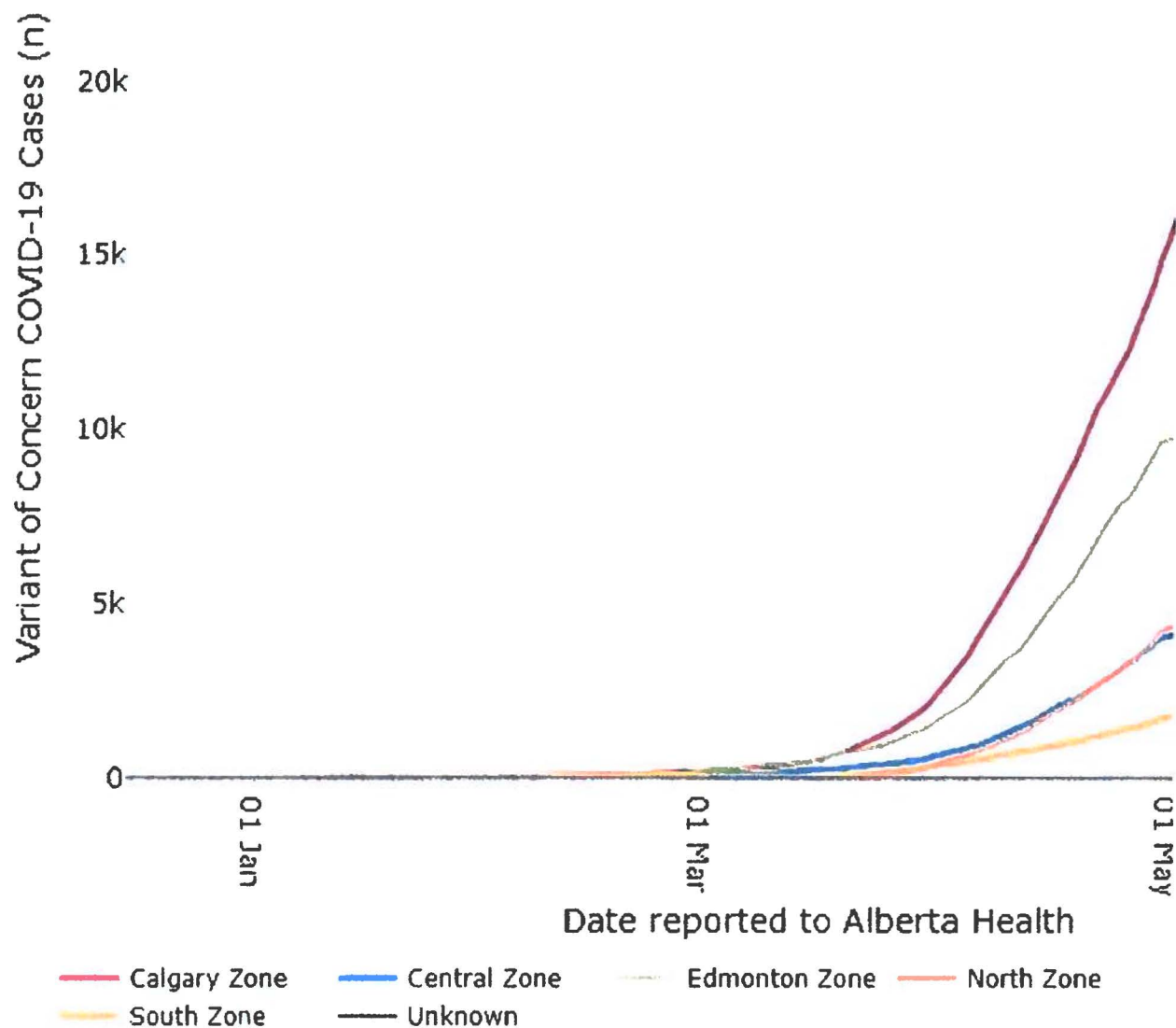


NE
Applicant
 This is Exhibit "M" referred to in the Affidavit of Kimberley Simmonds
 Sworn before me this 11th day of July, A.D., 2021

 A Notary Public, A Commissioner for Oaths in and for the Province of Alberta
Nick Parker
 Barrister & Solicitor

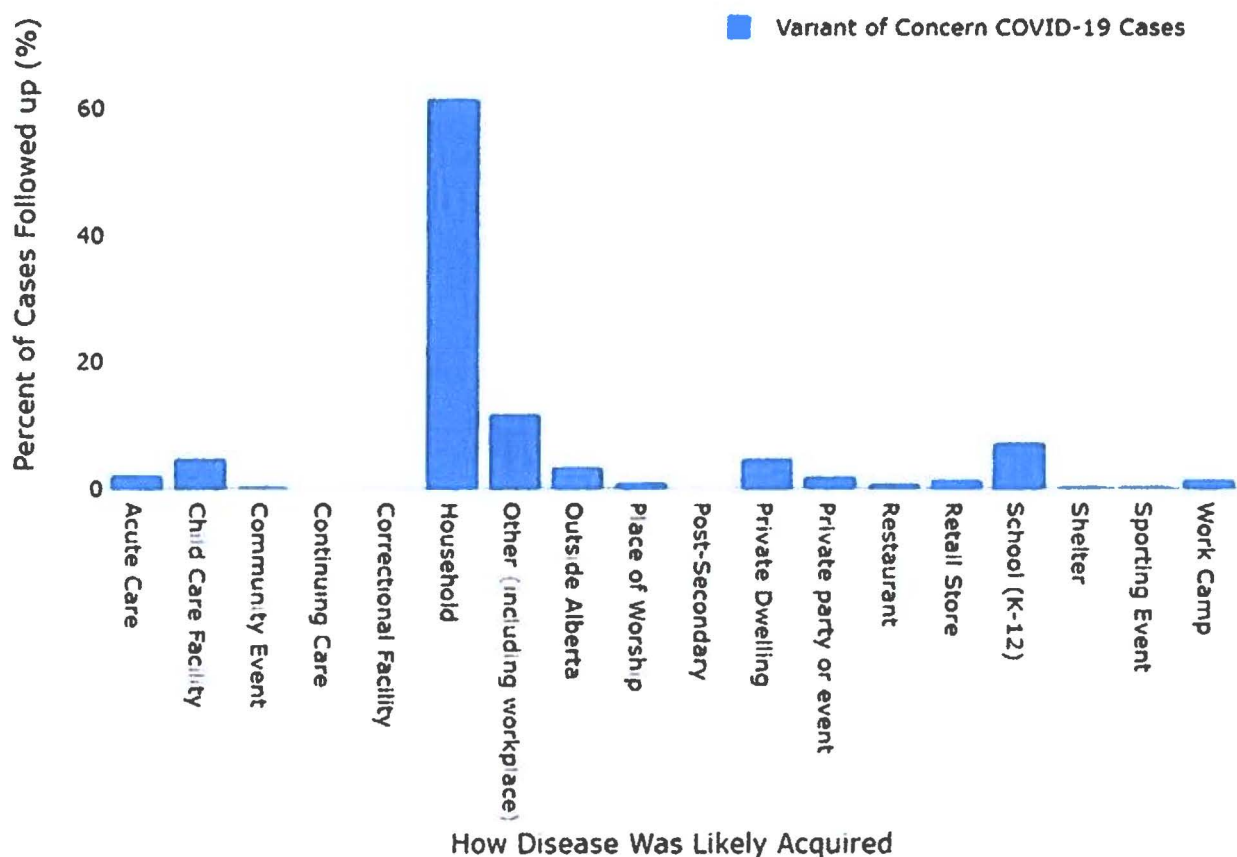
COVID-19 – Variants of Concern

All of the health zones in Alberta are have VOC cases, and transmission is occurring across the province. The Calgary Zone has experienced a disproportional number of cases and the resulting third wave has impacted the Calgary Zone more than other parts of the province.



COVID-19 – Variants of Concern

The increased transmission of the VOCs makes household attack rates higher than with the wild type. This aligns to the findings of other nationally and internationally^{1,2}. The high household transmission rates make it critical to minimize outbreaks as a case produced from those outbreaks can lead to entire households becoming infected.



¹ Increased household secondary attacks rates with Variant of Concern SARS-CoV-2 index cases

Sarah A. Buchan, Semra Tibebe, Nick Daneman, Michael Whelan, Thuva Vanniyasingam, Michelle Murti, Kevin A. Brown
medRxiv 2021.03.31.21254502; doi: <https://doi.org/10.1101/2021.03.31.21254502>

² Increased transmissibility of the B.1.1.7 SARS-CoV-2 variant: Evidence from contact tracing data in Oslo, January to February 2021. Jonas Christoffer Lindstrøm, Solveig Engebretsen, Anja Bråthen Kristoffersen, Gunnar Øyvind Isaksson Rø, Alfonso Diz-Lois Palomares, Kenth Engø-Monsen, Elisabeth Henie Madslien, Frode Forland, Karin Maria Nygård, Frode Hagen, Gunnar Gantzel, Ottar Wiklund, Arnoldo Frigessi, Birgitte Freiesleben de Blasio
medRxiv 2021.03.29.21254122; doi: <https://doi.org/10.1101/2021.03.29.21254122>